

Finite element and box-method discretizations for fractional elliptic problems with quadrature and mass lumping*

Kelvin J. R. Almeida-Sousa[†] David Bolin[†] Alexandre B. Simas[†]

Abstract

We analyze numerical approximation of the fractional elliptic problem $L^\beta u = f$, $\beta > 0$, where L is a second-order self-adjoint elliptic operator with homogeneous Dirichlet or Neumann boundary conditions. The paper develops a unified conforming piecewise linear framework that covers both the standard finite element discretization and the box-method discretization of fractional powers. The key point is that the discrete fractional operator is defined with respect to an admissible inner product on the trial space. This includes, in particular, the standard L^2 inner product and the quadrature-based mass-lumped inner product, and we also identify a broader family of admissible inner products interpolating between these two realizations. Within this framework, we show that the mass-lumped choice yields the intrinsic fractional box discretization, namely the one obtained by taking fractional powers of the nonfractional box solution operator. For both the finite element and box-method realizations, we establish error estimates under natural consistency assumptions, making explicit the effect of load quadrature in the box case. The analysis applies directly to practical schemes and is supported by numerical experiments in one and two space dimensions.

Keywords: fractional elliptic operators, box method, finite volume method, mass lumping, quadrature error, finite element method

MSC (2020): 35R11, 65N08, 65N15, 65N30, 47A60

1 Introduction

We study numerical approximation of the fractional elliptic problem

$$\begin{cases} L^\beta u = f & \text{in } \mathcal{S}, \\ \mathcal{B}u = 0 & \text{on } \partial\mathcal{S}, \end{cases} \quad (1)$$

where $\mathcal{S} \subset \mathbb{R}^d$ is a bounded convex interval, polygon, or polyhedron, $d \in \{1, 2, 3\}$, $\beta > 0$, \mathcal{B} denotes either homogeneous Dirichlet or homogeneous Neumann boundary conditions, and

$$L = -\operatorname{div}(A\nabla) + \kappa^2.$$

Here $A \in W^{1,\infty}(\mathcal{S}; \mathbb{R}^{d \times d})$ is symmetric and uniformly elliptic, while $\kappa \in W^{1,\infty}(\mathcal{S})$ satisfies $\kappa \geq \kappa_0 > 0$. The fractional powers of L are defined by spectral functional calculus, and under these assumptions (1) has a unique solution $u_\beta = L^{-\beta} f$.

Problems of this form are now standard in numerical analysis, stochastic modeling, and scientific computing. Fractional powers of elliptic operators appear in nonlocal diffusion [5,

*Submitted to the editors DATE. This work was funded by funded by King Abdullah University of Science and Technology (KAUST) under Award No. ORFS-CRG11-2022-5015.

[†]Statistics Program, King Abdullah University of Science and Technology, Saudi Arabia (kelvinjhonson.silva@kaust.edu.sa, david.bolin@kaust.edu.sa, alexandre.simas@kaust.edu.sa).

12], in regularity theory for parabolic equations [25], in rational and sinc approximations of semigroups and resolvents [5, 19], and in Gaussian field models such as the Whittle–Matérn class and its generalizations; see, for example, [3, 4, 24]. In all of these settings, the central numerical question is how to approximate the inverse fractional power $L^{-\beta}$ accurately and computationally efficiently.

At the continuous level, the problem is based on the coercive bilinear form

$$a(u, v) = \int_{\mathcal{S}} A \nabla u \cdot \nabla v \, dx + \int_{\mathcal{S}} \kappa^2 uv \, dx, \quad u, v \in \mathcal{V}, \quad (2)$$

where $\mathcal{V} = H_0^1(\mathcal{S})$ in the Dirichlet case and $\mathcal{V} = H^1(\mathcal{S})$ in the Neumann case. On a conforming simplicial mesh \mathcal{T}_h , letting $V_h \subset \mathcal{V}$ denote the standard continuous piecewise affine space, the classical P_1 finite element method (FEM) for the nonfractional problem seeks $u_h^{\text{fe}} \in V_h$ such that

$$a(u_h^{\text{fe}}, \chi) = (f, \chi), \quad \chi \in V_h. \quad (3)$$

This is also the natural starting point for fractional discretization: once a discrete elliptic operator has been defined on V_h , its fractional powers may be defined by finite-dimensional spectral calculus.

Indeed, several numerical approaches have been developed for fractional elliptic problems, which typically combine FEM approximation with an approximation of the fractional power, including quadrature-based methods [5], rational approximation methods [3, 4], and higher-dimensional extension techniques [16] based on the framework introduced by Caffarelli and Silvestre [7].

The issue we are investigating in this work is that the idealized formulation (3) is usually not the one that is actually assembled. In computation, the stiffness matrix, the mass matrix, and the load vector are typically obtained by numerical quadrature. Thus the implemented scheme often replaces the exact bilinear form by a quadrature-based bilinear form and replaces the exact L^2 pairing by a quadrature-based inner product; in particular, the latter includes the classical mass-lumping construction, in which the mass matrix is replaced by a diagonal quadrature-based approximation, see e.g., [6, 10, 27]. For the nonfractional problem, such modifications are classical variational crimes in the sense of Strang and Fix [26, Chapter 4]. For fractional powers, however, they play a more structural role. Once the discrete approximation is defined by taking a fractional power of a finite-dimensional operator, the bilinear form used to define that operator and the inner product used to realize it on V_h both affect the operator whose fractional power is being computed. It is therefore unclear how the theory developed in the nonfractional case transfers to the fractional problem.

This motivates the present work, where we analyze the approximation that is actually computed, rather than the ideal exact-integration Galerkin discretization. We study how the fractional discrete approximation depends on three ingredients:

- (a) the discrete bilinear form used to approximate the elliptic operator,
- (b) the discretization of the load term, and
- (c) the inner product used to realize the discrete operator on the trial space.

This issue is especially relevant in statistics. In the SPDE approach [24], Gaussian random fields are represented as solutions to elliptic or fractional elliptic equations driven by Gaussian white noise. In that setting, mass lumping and related approximations of the L^2 inner product are important as they replace dense mass matrices by diagonal surrogates, thereby inducing sparse precision operators and enabling scalable inference. The same principle also underlies more recent rational and covariance-based approximations of fractional SPDE models; see [3, 4]. Thus, the present paper is motivated both by how FEM approximations are assembled

in practice and by the need for sparse, implementable fractional discretizations in stochastic modeling.

To treat these issues, it is useful to compare FEM with the finite volume method (FVM) and with the box method. A finite volume method starts from local conservation: one introduces control volumes C and imposes balance laws of the form

$$-\int_{\partial C} A \nabla u_h \cdot n_C dS + \int_C \kappa^2 u_h dx = \int_C f dx \quad (4)$$

for every control volume C , where n_C is the outward unit normal on ∂C ; see, e.g., [8, 21].

This viewpoint naturally incorporates cellwise averaging of the load and gives a direct local interpretation for the nonfractional problem. For fractional powers, however, the situation is substantially more delicate. One can certainly take the matrix produced by a finite-volume method and apply a fractional power to it. But this operation is no longer tied directly to the local balance law (4).

More importantly, the resulting matrix function need not be a consistent discretization of the fractional power of the continuous operator.

Indeed, $L^{-\beta}$ is itself a global spectral object, and its discretization depends not only on the entries of a stiffness matrix, but also on the Hilbert-space realization with respect to which the discrete operator is selfadjoint. Thus, to obtain a meaningful fractional discretization, one needs more than local conservation: one needs a discrete operator that approximates the continuous selfadjoint realization of L in a compatible inner product, so that the spectral functional calculus is stable under discretization. This motivates the use of conservative discretizations that also admit a global symmetric representation on a conforming space. That keeps the finite-volume load averaging and local conservation structure of the nonfractional problem, while providing the Hilbert-space and spectral structure needed to define and analyze fractional powers. This is the perspective that leads to the box method.

The box method combines the two viewpoints. It is the vertex-centered control-volume discretization with conforming piecewise linear trial functions on the primal mesh and piecewise constant test functions on the associated barycentric dual mesh; see, for example, [2, 18, 20]. Hence, it preserves the conservative structure of a finite volume scheme while still working on the conforming finite element space V_h . This makes it especially suitable for the present problem: it allows one to define fractional powers on a conforming discrete space, to incorporate quadrature effects in the elliptic operator, and at the same time to retain control-volume averaging of the load.

More precisely, if $\mathcal{Z}_h^{\text{act}}$ denotes the active vertex set, $\{\phi_z\}_{z \in \mathcal{Z}_h^{\text{act}}}$ is the nodal basis of V_h , and if b_z is the barycentric dual cell associated with the vertex z , we define

$$V_{0,h} = \text{span}\{\mathbb{1}_{b_z} : z \in \mathcal{Z}_h^{\text{act}}\}, \quad (5)$$

and the transfer operator

$$Q : V_h \rightarrow V_{0,h}, \quad Q\chi = \sum_{z \in \mathcal{Z}_h^{\text{act}}} \chi(z) \mathbb{1}_{b_z}, \quad \chi = \sum_{z \in \mathcal{Z}_h^{\text{act}}} \chi(z) \phi_z \in V_h. \quad (6)$$

Thus $Q\chi$ is the piecewise constant function on the dual mesh that takes the nodal value $\chi(z)$ on b_z . Since $\{\phi_z\}_{z \in \mathcal{Z}_h^{\text{act}}}$ and $\{\mathbb{1}_{b_z}\}_{z \in \mathcal{Z}_h^{\text{act}}}$ are bases of spaces with the same dimension, Q is a linear isomorphism from V_h onto $V_{0,h}$. Moreover, although the diffusion coefficient A is assumed to belong to $W^{1,\infty}(\mathcal{S}; \mathbb{R}^{d \times d})$ and is therefore continuous, it is convenient to introduce the box bilinear form for a general bounded matrix field $B \in L^\infty(\mathcal{S}; \mathbb{R}^{d \times d})$. This allows us to cover, in particular, discontinuous coefficient fields arising from elementwise averaging or quadrature-based approximations. Hence, for a bounded matrix field $B \in L^\infty(\mathcal{S}; \mathbb{R}^{d \times d})$, we define the box

bilinear form

$$a_h^B(\chi, \psi) = - \sum_{z \in \mathcal{Z}_h^{\text{act}}} \psi(z) \int_{\partial b_z} B \nabla \chi \cdot \eta \, dS + \int_S \kappa^2 Q \chi Q \psi \, dx, \quad \chi, \psi \in V_h, \quad (7)$$

where η denotes the outward unit normal on ∂b_z . Intuitively, a_h^B is obtained by writing the flux-balance equation on each dual control volume, multiplying the balance on b_z by the nodal weight $\psi(z)$, and summing over all active vertices. In this way, the box method is a conservative finite-volume discretization written on the conforming finite element space V_h . Its nonfractional version reads: find $u_h^{\text{box}} \in V_h$ such that

$$a_h^A(u_h^{\text{box}}, \chi) = (f, Q\chi), \quad \chi \in V_h. \quad (8)$$

The point of the present paper is that, once fractional powers are introduced, one must keep separate the discrete bilinear form, the load discretization, and the inner product on V_h . Our goal is to analyze precisely this dependence.

To do so, we introduce a class of *admissible* inner products on V_h , broad enough to include the exact L^2 product, the quadrature-based mass-lumped product, and explicit banded families of inner products. We then study fractional finite-element and box-method discretizations in a common operator framework.

Our main contributions are the following.

- (i) We formulate a unified operator framework for finite-element and box-method discretizations of $L^{-\beta}$ in which the discrete bilinear form, the load discretization, and the inner product on V_h are kept separate.
- (ii) We introduce a broad class of admissible inner products that includes the exact L^2 product, the lumped-mass product, and explicit banded families of inner products, including the interpolation family of [28]. Thus the theory applies to practical sparse implementations, not only to ideal exact-integration schemes, and in particular to constructions that produce banded mass matrices relevant for efficient computation in SPDE-based statistical models.
- (iii) We show that the lumped-mass inner product is distinguished among all admissible inner products: For this choice, the fractional box discretization can be reconstructed directly from the nonfractional box solution operator.
- (iv) We prove error estimates for both FEM and box-method fractional discretizations under natural second-order consistency assumptions on the bilinear form and the inner product used on V_h . The finite-element scheme retains the classical order of convergence for fractional FEM, while the box-method scheme exhibits the expected loss caused by replacing the exact load functional by control-volume averaging. As a consequence, the convergence order is not affected by the efficiency enhancements that may arise from (a), (b) and (c).
- (v) We show that the proposed method can be combined with any exponentially convergent approximation method for the discrete operator, such as rational approximation or sinc quadrature, to obtain a fully implementable method with theoretical guarantees.

The analysis combines three ingredients. First, the barycentric box construction yields an exact local flux identity for cellwise constant coefficients, which leads to a coercivity theorem in dimensions $d = 1, 2, 3$. Second, the dependence on the auxiliary inner product is handled at the operator level rather than being hidden in matrices. Third, the error analysis separates the perturbation of the bilinear form from the perturbation of the load term, which makes it possible to identify precisely which part of the convergence rate comes from approximating the elliptic operator and which part comes from the box discretization of the right-hand side.

The remainder of the paper is organized as follows. Section 2 introduces the mesh notation, the primal and dual meshes, the conforming P_1 space, and the nonfractional box method. Section 3 defines the finite-element and box-method fractional discretizations, introduces admissible inner products, and proves the lumped-mass characterization. Section 4 contains the convergence analysis. Section 5 reports numerical experiments. Appendix A contains some of the longer proofs.

2 Finite elements, finite volumes, and the box method

We begin by introducing the concepts required for the box method in the non-fractional case $\beta = 1$, which is the foundation for the general fractional problem discussed in Section 3.

Recall that $\mathcal{V} = H_0^1(\mathcal{S})$ for homogeneous Dirichlet conditions and $\mathcal{V} = H^1(\mathcal{S})$ for homogeneous Neumann conditions, and let \mathcal{V}' denote the topological dual of \mathcal{V} . We write $\mathcal{H} = L^2(\mathcal{S})$, $\|v\| = \|v\|_{L^2(\mathcal{S})}$, $|v|_1 = \|\nabla v\|_{L^2(\mathcal{S})}$, and $\|v\|_{H^1(\mathcal{S})}^2 = \|v\|^2 + |v|_1^2$. Further, we use the notation \lesssim to denote inequalities that hold up to a constant independent of h , and \simeq to denote two-sided inequalities.

2.1 Primal and dual meshes

Let $\{\mathcal{T}_h\}_{h \downarrow 0}$ be a conforming family of simplicial triangulations of $\bar{\mathcal{S}}$. For each element $K \in \mathcal{T}_h$, write $h_K = \text{diam } K$ and let ρ_K be the diameter of the largest ball contained in K . The family is *shape regular* if there exists $\sigma_{\text{sr}} > 0$ such that

$$\rho_K \geq \sigma_{\text{sr}} h_K, \quad K \in \mathcal{T}_h, \quad h > 0. \quad (9)$$

We also write $h = \max_{K \in \mathcal{T}_h} h_K$. In Section 4 we will additionally assume quasi-uniformity, namely that there exists $\sigma_{\text{qu}} > 0$ such that $\sigma_{\text{qu}} h \leq h_K \leq h$ for all $K \in \mathcal{T}_h$.

Let \mathcal{Z}_h be the set of mesh vertices, let $\mathcal{Z}_h^{\text{bd}} = \mathcal{Z}_h \cap \partial\mathcal{S}$, and let $\mathcal{Z}_h^{\text{in}} = \mathcal{Z}_h \setminus \mathcal{Z}_h^{\text{bd}}$. The set of active vertices is

$$\mathcal{Z}_h^{\text{act}} = \begin{cases} \mathcal{Z}_h^{\text{in}} & \text{in the Dirichlet case,} \\ \mathcal{Z}_h & \text{in the Neumann case.} \end{cases}$$

The trial space is the conforming piecewise affine space

$$V_h = \text{span}\{\phi_z : z \in \mathcal{Z}_h^{\text{act}}\} \subset \mathcal{V},$$

where ϕ_z denotes the standard nodal basis function associated with z . Equivalently, V_h is the image of the global Lagrange interpolant associated with \mathcal{T}_h ; see [6, Definition 3.3.9]. Thus V_h is the usual P_1 finite-element space with the boundary condition built into the choice of active vertices.

As explained in the introduction, the box method keeps the conforming trial space V_h and uses barycentric dual cells as control volumes. To define the dual mesh, fix $K \in \mathcal{T}_h$ and let $\mathcal{Z}(K)$ denote the set of vertices of K . For each $z \in \mathcal{Z}(K)$, we construct a region $\mathcal{A}_z(K) \subset K$ as follows. We consider all k -dimensional faces of K , for $0 \leq k \leq d$, that contain z , and collect their barycenters. Thus, this collection includes the vertex z itself (viewed as a 0-dimensional face), the barycenters of all edges containing z , the barycenters of all higher-dimensional faces containing z , and the barycenter of K itself. If q_1, \dots, q_{M_h} denotes an enumeration of these barycenters other than z , we define $\mathcal{A}_z(K) = \text{co}(z, q_1, \dots, q_{M_h})$, where $\text{co}(\cdot)$ denotes the convex hull. See Figure 1 for an illustration of this construction. The family $\{\mathcal{A}_z(K)\}_{z \in \mathcal{Z}(K)}$ partitions K into $d + 1$ subregions of equal d -dimensional Lebesgue measure. The dual control volume associated with an active vertex z is then

$$b_z = \bigcup_{K \in \mathcal{T}_h: z \in K} \mathcal{A}_z(K).$$

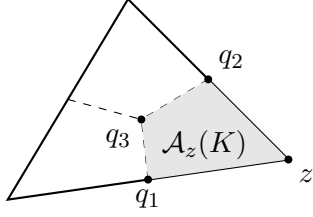


Figure 1: Polygonal region $\mathcal{A}_z(K)$, in the case $d = 2$, where q_1 and q_2 are the barycenter (midpoints) of the edges that contains z and q_3 is the barycenter of K itself.

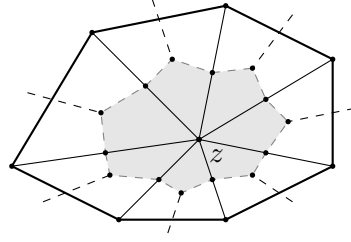


Figure 2: Dual element $b_z \in \mathcal{B}$, corresponding to $z \in \mathcal{Z}^{in}$ in the case $d = 2$.

The set $\mathcal{B} = \{b_z\}_{z \in \mathcal{Z}_h^{\text{act}}}$ forms the vertex-centered dual mesh used by the box method; see also [2, 8, 21]. Figure 2 illustrates the construction for $d = 2$.

2.2 The box method, the box bilinear form, and the load operator

We now specialize the finite volume construction to the barycentric dual mesh. Recall from (7) that the box bilinear form a_h^A is obtained by transporting local flux balances on the dual cells b_z to the conforming space V_h . We now make this explicit.

For $u_h \in V_h$, the local balance on the dual cell b_z reads

$$-\int_{\partial b_z} A \nabla u_h \cdot \eta \, dS + \int_{b_z} \kappa^2 Q u_h \, dx = \int_{b_z} f \, dx, \quad z \in \mathcal{Z}_h^{\text{act}}. \quad (10)$$

Since $Q u_h$ is constant on b_z with value $u_h(z)$, the reaction term is the standard control-volume contribution. Thus (10) is the local finite-volume balance underlying the box method. Multiplying the balance on b_z by $\chi(z)$ and summing over all active vertices yields the variational formulation (7), and hence the nonfractional box method (8).

We begin with the case in which B is piecewise constant on the primal mesh. In that situation, the flux representation of the box method reduces to a standard domain integral, which makes the symmetry of the form transparent and provides the basic structural identity used below.

Lemma 2.1. *Assume that $B \in L^\infty(\mathcal{S}; \mathbb{R}^{d \times d})$ is constant on each element $K \in \mathcal{T}_h$. Then, for all $\chi, \psi \in V_h$, the corresponding box bilinear form satisfies*

$$a_h^B(\chi, \psi) = \int_{\mathcal{S}} B \nabla \chi \cdot \nabla \psi \, dx + \int_{\mathcal{S}} \kappa^2 Q \chi Q \psi \, dx. \quad (11)$$

In particular, if B is symmetric, then a_h^B is symmetric.

Although stated for piecewise-constant coefficient fields, (11) connects directly to the variable-coefficient setting. Indeed, if A is replaced by its elementwise average on each $K \in \mathcal{T}_h$, then one obtains a box bilinear form satisfying an identity of the same type. We record this consequence separately, since it yields an explicit symmetric example within the class of box bilinear forms covered by our fractional framework.

Lemma 2.2. *Let $\kappa \in W^{1,\infty}(\mathcal{S})$ and A_h be the piecewise-constant matrix field defined on each element $K \in \mathcal{T}_h$ by $A_h|_K = \frac{1}{|K|} \int_K A(x) \, dx$. Then, for all $\chi, \psi \in V_h$,*

$$a_h^{A_h}(\chi, \psi) = \int_{\mathcal{S}} A_h \nabla \chi \cdot \nabla \psi \, dx + \int_{\mathcal{S}} \kappa^2 Q \chi Q \psi \, dx. \quad (12)$$

In particular, $a_h^{A_h}$ is symmetric.

We next state the coercivity result for the physical coefficient field A . The proof is given in Appendix A.

Theorem 2.3. *Assume $d \in \{1, 2, 3\}$, $A \in W^{1,\infty}(\mathcal{S}; \mathbb{R}^{d \times d})$, and that $A(x)$ is symmetric and uniformly elliptic. Let A_h be as in Lemma 2.2. Then there exist $c > 0$ and $h_0 > 0$, independent of h , such that*

$$a_h^A(\chi, \chi) \geq c \|\chi\|_{H^1(\mathcal{S})}^2 \quad \text{and} \quad a_h^{A_h}(\chi, \chi) \geq c \|\chi\|_{H^1(\mathcal{S})}^2, \quad \chi \in V_h, \quad 0 < h < h_0. \quad (13)$$

By the discussion in the introduction regarding the need for symmetric and global bilinear forms in order to naturally define fractional operators, we will consider the symmetric box problem, that is, box problem associated to A_h . By Theorem 2.3, the symmetric nonfractional box problem

$$a_h^{A_h}(u_h, \chi) = (f, Q\chi), \quad \chi \in V_h, \quad (14)$$

has a unique solution for all sufficiently small h . We denote the associated nonfractional box solution operator by

$$T_h^{\text{box}} : L^2(\mathcal{S}) \rightarrow V_h, \quad a_h^{A_h}(T_h^{\text{box}} f, \chi) = (f, Q\chi), \quad \chi \in V_h. \quad (15)$$

This is the discrete solution operator of the box method. For the moment we keep this concrete notation, since it is the nonfractional box operator that underlies the later fractional construction. In the next step we pass to a more general operator framework, in which the box method appears as one particular realization.

To express (15) in operator form, and later extend it to fractional powers, we must specify how the discrete operator is realized on V_h . This requires an inner product on V_h . Let $\langle \cdot, \cdot \rangle_h$ be an inner product on V_h , and write $\|\chi\|_h = \langle \chi, \chi \rangle_h^{1/2}$. Given a symmetric bilinear form a_h on V_h , we define the operators $L_h : V_h \rightarrow V_h$, $P_h : L^2(\mathcal{S}) \rightarrow V_h$, and $\Lambda_h : L^2(\mathcal{S}) \rightarrow V_h$ through

$$\langle L_h \chi, \psi \rangle_h = a_h(\chi, \psi), \quad \langle P_h f, \chi \rangle_h = (f, Q\chi), \quad \langle \Lambda_h f, \chi \rangle_h = (f, \chi), \quad (16)$$

for $\chi, \psi \in V_h$ and $f \in L^2(\mathcal{S})$. The operator P_h is the load operator associated with the box method, since it acts against the piecewise constant test function $Q\chi$, whereas Λ_h is the corresponding finite-element load operator. In particular, when $a_h = a_h^{A_h}$, the solution operator in (15) takes the form $T_h^{\text{box}} = L_h^{-1} P_h$. More generally, whenever a_h is coercive on V_h , we write $T_h = L_h^{-1} P_h$ for the corresponding nonfractional box solution operator.

In the nonfractional case, the auxiliary inner product enters only through the operator representation. Indeed, the equation $L_h u_h = P_h f$ is equivalent to the variational formulation

$$a_h(u_h, \chi) = (f, Q\chi), \quad \chi \in V_h,$$

and therefore the resulting function $u_h \in V_h$ is independent of the particular Riesz map induced by $\langle \cdot, \cdot \rangle_h$. For fractional powers, the situation changes. The operator $L_h^{-\beta}$ is defined through the spectral calculus of L_h as an operator on the Hilbert space $(V_h, \langle \cdot, \cdot \rangle_h)$. Consequently, the inner product is no longer only a representational choice; it becomes part of the discrete fractional operator. We therefore restrict attention to inner products that are uniformly equivalent and consistent with the L^2 inner product, and to symmetric bilinear forms that are uniformly consistent with the continuous form a . This leads to the following definitions.

Definition 2.4 (Admissible inner product). An inner product $\langle \cdot, \cdot \rangle_h$ on V_h is called *admissible* if the following estimates hold uniformly in h :

$$(i) \quad |(\chi, \psi) - \langle \chi, \psi \rangle_h| \lesssim h^2 |\chi|_1 |\psi|_1, \quad \chi, \psi \in V_h;$$

(ii)

$$\|\chi\|_h \simeq \|\chi\|, \quad \chi \in V_h.$$

Definition 2.5 (Admissible bilinear form). A symmetric bilinear form a_h on V_h is *admissible* if it is continuous on $V_h \times V_h$ and satisfies the consistency estimate

$$|a(\chi, \psi) - a_h(\chi, \psi)| \lesssim h^2 |\chi|_1 |\psi|_1, \quad \chi, \psi \in V_h, \quad (17)$$

uniformly in h .

Remark 2.6. Every admissible bilinear form is coercive on V_h for sufficiently small h . Indeed, since $a(\cdot, \cdot)$ is coercive on $\mathcal{V} \supset V_h$, Definition 2.5 gives

$$a_h(\chi, \chi) \geq a(\chi, \chi) - Ch^2 |\chi|_1^2 \geq c \|\chi\|_{H^1(\mathcal{S})}^2$$

for all $\chi \in V_h$ and all sufficiently small h .

The following examples show that the class of admissible inner products includes the standard choices used in practice.

Example 2.7. The following three inner products will be used repeatedly.

- (i) the exact $L^2(\mathcal{S})$ inner product $\langle \chi, \psi \rangle_h = (\chi, \psi)$,
- (ii) the mixed inner product $\langle \chi, \psi \rangle_h = (\chi, Q\psi) = \sum_{z, w \in \mathcal{Z}_h^{\text{act}}} \chi(z) \psi(w) \int_{b_w} \phi_z(x) dx$, where ϕ_z denotes the nodal basis of V_h and b_w is the corresponding element of the dual mesh;
- (iii) the lumped-mass inner product $\langle \chi, \psi \rangle_h = (Q\chi, Q\psi) = \sum_{z \in \mathcal{Z}_h^{\text{act}}} \chi(z) \psi(z) |b_z|$.

Their associated norms are uniformly equivalent to the $L^2(\mathcal{S})$ norm on V_h .

All inner products in Example 2.7 are admissible in the sense of Definition 2.4; see, e.g., [8, 13, 27]. Further non-trivial examples of admissible inner products will be provided in Proposition 3.7.

We next record some elementary properties of the box load operator. These facts are independent of the fractional construction, but they clarify the role of P_h and will be used later. In particular, they show that P_h behaves like a projection only in a very restricted sense.

Proposition 2.8. *Let P_h and Λ_h be defined by (16). Then*

- (i) $P_h = P_h \Pi_{0,h}$, where $\Pi_{0,h}$ is the $L^2(\mathcal{S})$ -orthogonal projector onto $V_{0,h}$;
- (ii) If there exists $C > 0$, independent of h , such that $\|Q\chi\| \leq C \|\chi\|_h$ for all $\chi \in V_h$, then $P_h : L^2(\mathcal{S}) \rightarrow V_h$ is bounded and $\|P_h f\|_h \leq C \|f\|$;
- (iii) $\ker P_h = \{f \in L^2(\mathcal{S}) : \Pi_{0,h} f|_{b_z} = 0 \text{ for all } z \in \mathcal{Z}_h^{\text{act}}\}$ and $\text{ran } P_h = V_h$;
- (iv) The $L^2(\mathcal{S})$ -adjoint of P_h is $P_h^* = Q\Lambda_h$.

The proof is routine after writing $\Pi_{0,h} f$ in the dual-cell basis and using the defining relations in (16). The detailed argument is given in Appendix A. Since $\|Q\chi\| \simeq \|\chi\|$ on V_h , Definition 2.4(ii) implies that the boundedness assumption in item (ii) holds for every admissible inner product.

The next corollary makes precise the limited sense in which P_h can be regarded as a projection. It is a projection only for the mixed inner product, and even then it is not an orthogonal projection on $L^2(\mathcal{S})$.

Corollary 2.9. *The operator P_h is a projection if and only if $\langle \chi, \psi \rangle_h = (\chi, Q\psi)$ for all $\chi, \psi \in V_h$. Even in that case, P_h is not an orthogonal projection on $L^2(\mathcal{S})$.*

Corollary 2.9 follows as a consequence of Proposition 2.8(iv). For a detailed proof, see Appendix A.

The box bilinear form (7) arises from local flux balances on the dual cells, a structure natural for the nonfractional problem.

However, as will be seen in Section 3, fractional powers are defined through the associated discrete operator and therefore depend on its global structure rather than on individual control-volume balances.

This is why, in the present setting, we seek box-method bilinear forms that admit a global representation on V_h . Moreover, in view of Definition 2.5, we require these forms to be symmetric, so that the induced discrete operator is selfadjoint and the spectral calculus can be applied to define its fractional powers.

Lemma 2.2 provides a first example of this mechanism: when A is replaced by its elementwise average, the local box form (7) can be rewritten in the global form (12). More generally, the class of bilinear forms relevant for our fractional box-method includes both such averaged-coefficient constructions and fully quadrature-based global approximations, as illustrated next.

Example 2.10. Two basic examples of admissible box-method bilinear forms with global representations are the following.

- (a) If A_h denotes the elementwise average of A , then Lemma 2.2 shows that the corresponding box bilinear form admits the global representation (12). In particular, it is symmetric and therefore fits naturally into the operator framework used later for fractional powers.
- (b) A fully quadrature-based example is obtained by using Q as a quadrature rule on the box bilinear form $a_h^{A_h}$. On each element K , this rule is exact for affine functions and second-order accurate for smooth integrands. For example, a sufficient condition is $A \in W^{1,\infty}(\mathcal{S}; \mathbb{R}^{d \times d})$ and $\kappa \in W^{2,\infty}(\mathcal{S})$, see e.g. [14] and [23, Lemma 2.3]. This leads to the global bilinear form

$$a_h(\chi, \psi) = Q(A \nabla \chi \cdot \nabla \psi) + Q(\kappa^2 \chi \psi). \quad (18)$$

This form is written directly as a global quadrature approximation of the continuous bilinear form (2). When symmetric, it also induces a selfadjoint discrete operator, and is therefore equally suitable for the spectral definition of fractional powers. By the standard quadrature-error estimates of Strang and Fix [14, 26] and the FEM bounds in [27], this choice satisfies Definition 2.5.

3 Fractional finite-element and box-method discretizations

By the assumptions on A and κ , the bilinear form a in (2) is continuous and coercive on \mathcal{V} . Hence there exists an isomorphism $L : \mathcal{V} \rightarrow \mathcal{V}'$ such that

$$\langle Lu, v \rangle_{\mathcal{V}' \times \mathcal{V}} = a(u, v), \quad u, v \in \mathcal{V}.$$

When realized on $L^2(\mathcal{S})$, the operator L is positive, selfadjoint, and has compact inverse. Let $\{(\lambda_j, \varphi_j)\}_{j \geq 1}$ be the corresponding $L^2(\mathcal{S})$ -orthonormal eigensystem.

For $s \geq 0$, we define fractional power of L by spectral calculus: for $v \in D(L^{s/2})$, $L^{s/2}v = \sum_{j \geq 1} \lambda_j^{s/2} (v, \varphi_j) \varphi_j$, where

$$\dot{H}^s := D(L^{s/2}) = \left\{ v \in L^2(\mathcal{S}) : \sum_{j \geq 1} \lambda_j^s |(v, \varphi_j)|^2 < \infty \right\}, \quad \|v\|_s^2 := \sum_{j \geq 1} \lambda_j^s |(v, \varphi_j)|^2. \quad (19)$$

For $s < 0$, we define \dot{H}^s as the completion of $L^2(\mathcal{S})$ with respect to the norm in (19); equivalently, \dot{H}^s is the dual of \dot{H}^{-s} with $L^2(\mathcal{S})$ as pivot space. This is the scale that will be used throughout the paper. In particular, if $f \in L^2(\mathcal{S})$ and $\beta > 0$, then

$$u_\beta = L^{-\beta} f \in \dot{H}^{2\beta} \quad \text{and} \quad \|u_\beta\|_{2\beta} = \|f\|.$$

The error estimates proved later are measured in the norms $\|\cdot\|_\delta$ with $0 \leq \delta \leq 1$.

We now pass from the nonfractional FEM and box schemes to their fractional analogues. The key bookkeeping point is that three ingredients must be kept separate: the symmetric bilinear form a_h , the auxiliary inner product $\langle \cdot, \cdot \rangle_h$ used to realize the discrete operator on V_h , and the load operator P_h . For $\beta = 1$ this distinction is largely hidden because the solution is recovered from a variational equation. For $\beta \neq 1$, by contrast, the functional calculus is applied directly to the discrete operator, so the choice of Riesz map becomes part of the approximation.

From now on a_h denotes an admissible symmetric bilinear form in the sense of Definition 2.5 and $\langle \cdot, \cdot \rangle_h$ denotes an admissible inner product in the sense of Definition 2.4. The corresponding discrete operator $L_h : V_h \rightarrow V_h$ is defined by (16); by Remark 2.6, L_h is positive and selfadjoint on the Hilbert space $(V_h, \langle \cdot, \cdot \rangle_h)$ for all sufficiently fine meshes, so $L_h^{-\beta}$ is well defined by the spectral theorem for every $\beta > 0$. Because L_h is finite dimensional and positive, the operator $L_h^{-\beta}$ also admits the standard holomorphic contour representation, see [17].

The finite-element fractional discretization based on an admissible inner product $\langle \cdot, \cdot \rangle_h$ is the direct Galerkin analogue of the classical fractional FEM construction and serves as the reference scheme against which the box discretization will be compared. It is given, in terms of our discrete operators, by

$$\bar{u}_{\beta,h} = L_h^{-\beta} \Lambda_h f. \quad (20)$$

The box fractional discretization keeps the same discrete operator but replaces the exact $L^2(\mathcal{S})$ load projector by the box load operator P_h , thereby retaining the control-volume averaging that characterizes the box method already at the nonfractional level.

Definition 3.1. For $\beta > 0$, the *box-method fractional discretization* associated with a_h and $\langle \cdot, \cdot \rangle_h$ is

$$u_{\beta,h} = T_{h,\beta} f := L_h^{-\beta} P_h f. \quad (21)$$

When $\beta = 1$, this reduces to the nonfractional discrete solution operator $T_h = L_h^{-1} P_h$.

Remark 3.2. For $\beta = 1$, the discrete solution operator $T_h = L_h^{-1} P_h$ is independent of the auxiliary inner product on V_h . Indeed, the equation $L_h u_h = P_h f$ is equivalent to the variational statement

$$a_h(u_h, \chi) = (f, Q\chi), \quad \chi \in V_h,$$

which involves neither the Riesz map of $\langle \cdot, \cdot \rangle_h$ nor the representation matrices of L_h and P_h . For $\beta \neq 1$, the functional calculus is performed on L_h itself, and the dependence on $\langle \cdot, \cdot \rangle_h$ becomes genuine.

3.1 Matrix representation and inner-product dependence

The preceding remark is transparent in coordinates. Fix the nodal basis $\{\phi_j\}_{j=1}^{N_h}$ of V_h and write $[\chi] \in \mathbb{R}^{N_h}$ for the coordinate vector of $\chi \in V_h$. Let $\mathbf{M}_h = (\langle \phi_j, \phi_i \rangle_h)_{i,j}$ and $\mathbf{K}_h = (a_h(\phi_j, \phi_i))_{i,j}$, and, for $f \in L^2(\mathcal{S})$, define $\mathbf{F}_Q(f) = ((f, Q\phi_i))_{i=1}^{N_h}$ and $\mathbf{F}(f) = ((f, \phi_i))_{i=1}^{N_h}$. The matrix \mathbf{M}_h depends on the chosen inner product, whereas \mathbf{K}_h depends only on a_h .

Proposition 3.3. *Let $\beta \in \{1, 2, 3, \dots\}$. With the notation above,*

$$[L_h \chi] = \mathbf{M}_h^{-1} \mathbf{K}_h [\chi], \quad [P_h f] = \mathbf{M}_h^{-1} \mathbf{F}_Q(f), \quad [\Lambda_h f] = \mathbf{M}_h^{-1} \mathbf{F}(f). \quad (22)$$

Consequently,

$$[u_{\beta,h}] = (\mathbf{M}_h^{-1}\mathbf{K}_h)^{-\beta}\mathbf{M}_h^{-1}\mathbf{F}_Q(f), \quad [\bar{u}_{\beta,h}] = (\mathbf{M}_h^{-1}\mathbf{K}_h)^{-\beta}\mathbf{M}_h^{-1}\mathbf{F}(f). \quad (23)$$

For $\beta = 1$, the dependence on \mathbf{M}_h cancels and

$$[u_{1,h}] = \mathbf{K}_h^{-1}\mathbf{F}_Q(f). \quad (24)$$

Proof. By definition, $\langle L_h\chi, \phi_i \rangle_h = a_h(\chi, \phi_i)$. Writing this relation in terms of coordinates, we obtain $\mathbf{M}_h[L_h\chi] = \mathbf{K}_h[\chi]$, which gives the first relation in (22). The other two follow from the definitions of P_h and Λ_h in the same way. Formula (23) is then immediate from Definitions 3.1 and (20), and (24) follows by setting $\beta = 1$. \square

Proposition 3.3 pinpoints the source of the difficulty: the nonfractional discrete solution depends only on \mathbf{K}_h and the associated load vector, whereas the fractional map depends on the similarity class of $\mathbf{M}_h^{-1}\mathbf{K}_h$. In this sense, once fractional powers are introduced, the inner product becomes part of the approximation itself. The same matrix perspective also makes clear that quadrature and mass lumping are not merely cosmetic implementation choices, but give rise to genuinely different discretizations of the same continuous problem.

A useful benchmark is the classical FEM discretization. If $\widehat{T}_h = \widehat{L}_h^{-1}\Pi_h$ denotes the nonfractional FEM solution operator associated with the exact form a and the exact $L^2(\mathcal{S})$ inner product, then \widehat{T}_h is selfadjoint and nonnegative on $L^2(\mathcal{S})$, and

$$(\widehat{T}_h)^\beta = \widehat{L}_h^{-\beta}\Pi_h, \quad \beta > 0. \quad (25)$$

Indeed, Π_h is the orthogonal projector onto the invariant subspace V_h and \widehat{L}_h is positive self-adjoint on V_h , so the spectral calculus may be performed either on \widehat{T}_h or on \widehat{L}_h . Identity (25) provides the finite-element analogue of the intrinsic construction we seek for the box method.

The next proposition explains why the operator QT_h is the natural box-method counterpart of \widehat{T}_h .

Proposition 3.4. *Let $T_h = L_h^{-1}P_h$ be the nonfractional box solution operator. Then $QT_h : L^2(\mathcal{S}) \rightarrow V_{0,h} \subset L^2(\mathcal{S})$ is selfadjoint and nonnegative.*

Proof. For any $f, g \in L^2(\mathcal{S})$, the defining relation for T_h gives

$$(f, QT_h g) = a_h(T_h f, T_h g) = a_h(T_h g, T_h f) = (g, QT_h f), \quad (26)$$

which shows that QT_h is self-adjoint. Taking $f = g$ in (26), we obtain $(f, QT_h f) = a_h(T_h f, T_h f) \geq 0$ and the nonnegativity of QT_h follows. \square

Proposition 3.4 shows that the nonfractional box solution operator already possesses the spectral structure needed to define fractional powers, but only after composition with Q . The remaining question is whether this construction can be brought back to the primal finite-element space without introducing an arbitrary auxiliary inner product. The next definition singles out the mass-lumped inner product and the next theorem shows that it is this choice that makes the fractional box discretization intrinsic, in the sense that it is determined by the nonfractional box solution operator.

Definition 3.5. Let $\langle \chi, \psi \rangle_Q = (Q\chi, Q\psi)$ be the lumped-mass inner product on V_h , and let $L_{h,Q}$ and $P_{h,Q}$ be the operators defined by (16) with this inner product. The corresponding *intrinsic box-method discretization* is

$$u_{\beta,h}^Q = T_{h,\beta}^Q f := (L_{h,Q})^{-\beta} P_{h,Q} f. \quad (27)$$

Theorem 3.6. For every $\beta > 0$,

$$T_{h,\beta}^Q = Q^{-1}(QT_h)^\beta, \quad (28)$$

where $T_h = L_h^{-1}P_h$ is the nonfractional box solution operator. In particular, $T_{h,\beta}^Q$ depends only on T_h and therefore, by Remark 3.2, is independent of the auxiliary inner product used to represent the nonfractional problem.

Proof. We work with the lumped-mass inner product. Also, recall that $\Pi_{0,h}$ is the $L^2(\mathcal{S})$ -orthogonal projector onto $V_{0,h}$. Since $Q : (V_h, \langle \cdot, \cdot \rangle_Q) \rightarrow (V_{0,h}, (\cdot, \cdot))$ is an isometric isomorphism, we have $Q^* = Q^{-1}$. Hence Q implements a unitary equivalence between these two Hilbert spaces, and therefore the operator

$$S_h = QL_{h,Q}^{-1}Q^{-1} : V_{0,h} \rightarrow V_{0,h}$$

is positive and selfadjoint on $V_{0,h}$. Moreover, for every $f \in L^2(\mathcal{S})$ and $\chi \in V_h$,

$$\langle P_{h,Q}f, \chi \rangle_Q = (f, Q\chi) = (\Pi_{0,h}f, Q\chi) = \langle Q^{-1}\Pi_{0,h}f, \chi \rangle_Q.$$

Since this holds for all $\chi \in V_h$, it follows that $P_{h,Q} = Q^{-1}\Pi_{0,h}$, and therefore

$$QT_h = QL_{h,Q}^{-1}P_{h,Q} = QL_{h,Q}^{-1}Q^{-1}\Pi_{0,h} = S_h^{-1}\Pi_{0,h}.$$

Recall that Q implements a unitary equivalence between $L_{h,Q}^{-1}$ on V_h and $S_h^{-1} = QL_{h,Q}^{-1}Q^{-1}$ on $V_{0,h}$. By the spectral calculus, fractional powers are preserved under unitary equivalence, and thus $S_h^{-\beta} = QL_{h,Q}^{-\beta}Q^{-1}$. Moreover, $\Pi_{0,h}$ is the $L^2(\mathcal{S})$ -orthogonal projector onto $V_{0,h}$, and S_h^{-1} is positive selfadjoint on $V_{0,h}$. Thus $S_h^{-1}\Pi_{0,h}$ is precisely the extension of S_h^{-1} to $L^2(\mathcal{S})$ by zero on $V_{0,h}^\perp$. Therefore, its fractional powers are given by the same extension of the fractional powers of S_h^{-1} , and hence

$$(QT_h)^\beta = (S_h^{-1}\Pi_{0,h})^\beta = S_h^{-\beta}\Pi_{0,h} = QL_{h,Q}^{-\beta}Q^{-1}\Pi_{0,h}.$$

Applying Q^{-1} and using again $P_{h,Q} = Q^{-1}\Pi_{0,h}$ yields

$$Q^{-1}(QT_h)^\beta = (L_{h,Q})^{-\beta}P_{h,Q} = T_{h,\beta}^Q.$$

This proves (28). □

Theorem 3.6 is the precise form of the structural statement announced in the introduction: among all admissible inner products, the lumped-mass choice is exactly the one that turns the box-method fractional discretization into a construction intrinsic to the nonfractional box solution operator.

We also retain the family of inner products proposed in [28]. Let $N_h = \dim V_h$ and let \mathbf{M} be the classical mass matrix, $\mathbf{M}_{ij} = (\phi_i, \phi_j)$.

Proposition 3.7. For $0 \leq i \leq N_h - 1$, decompose the mass matrix as $\mathbf{M} = \mathbf{D}_i + \mathbf{R}_i$, where \mathbf{D}_i contains the entries of \mathbf{M} within bandwidth i , and \mathbf{R}_i is the remainder. Let \mathcal{L} denote the mass-lumping operator, defined on a matrix \mathbf{A} by

$$\mathcal{L}(\mathbf{A})_{mn} = \delta_{mn} \sum_{k=1}^{N_h} \mathbf{A}_{mk},$$

where δ_{mn} is the Kronecker delta, and define $\mathbf{M}_i = \mathbf{D}_i + \mathcal{L}(\mathbf{R}_i)$. Then

$$\langle \chi, \psi \rangle_{i,h} = [\chi]^T \mathbf{M}_i [\psi], \quad \chi, \psi \in V_h, \quad (29)$$

defines an admissible inner product in the sense of Definition 2.4.

Proof. Given matrices $\mathbf{A}, \mathbf{B} \in \mathbb{R}^{N_h \times N_h}$, we write $\mathbf{A} \preceq \mathbf{B}$ (respectively, $\mathbf{A} \prec \mathbf{B}$) if $\mathbf{B} - \mathbf{A}$ is a non-negative semi-definite matrix (respectively, a positive definite matrix). By [28, Lemma 3.19] we have that if \mathcal{L} is the mass lumping operator, then

$$-\mathcal{L}(\mathbf{A}) \preceq \mathbf{A} \preceq \mathcal{L}(\mathbf{A}) \quad (30)$$

for every symmetric matrix with positive entries $\mathbf{A} \in \mathbb{R}^{N_h \times N_h}$. Observing that $\mathcal{L}(\mathbf{M}) = \mathcal{L}(\mathbf{M}_i) = \mathcal{L}(\mathbf{D}_i + \mathcal{L}(\mathbf{R}_i))$, it follows from (30) that

$$0 \prec \mathbf{M} = \mathbf{D}_i + \mathbf{R}_i \preceq \mathbf{D}_i + \mathcal{L}(\mathbf{R}_i) = \mathbf{M}_i \preceq \mathcal{L}(\mathbf{M}) \quad (31)$$

for every $0 \leq i \leq N_h - 1$. Since the norms induced by \mathbf{M} and $\mathcal{L}(\mathbf{M})$, in the sense of (29), correspond to the L^2 inner product and the lumped mass inner product over V_h , respectively, it follows from (31) that $\|\cdot\|_i := \sqrt{\langle \cdot, \cdot \rangle_i}$ is equivalent to $\|\cdot\|$, with bounding constants independent of h . Again, from (31), we have

$$0 \leq \|\phi\|_i^2 - \|\phi\|^2 \leq \|\phi\|_Q^2 - \|\phi\|^2 \lesssim h^2 |\phi|_1^2, \quad \forall \phi \in V_h, \quad (32)$$

where the last estimate holds due to [8, Lemma 5.1]. What remains is to extend (32) to the case of the inner product $\langle \cdot, \cdot \rangle_i$. To this end, define $a(\chi, \psi) := \langle \chi, \psi \rangle_i - (\chi, \psi)$ and note that a is bilinear, symmetric and, due to (32), $a(\chi, \chi) \geq 0$ for every $\chi \in V_h$. Under these hypotheses, Cauchy-Schwarz inequality holds for a , and we have

$$|\langle \chi, \psi \rangle_i - (\chi, \psi)| = |a(\chi, \psi)| \leq a(\chi, \chi)^{\frac{1}{2}} a(\psi, \psi)^{\frac{1}{2}} \lesssim h^2 |\chi|_1 |\psi|_1.$$

□

Remark 3.8. In Proposition 3.7, we have $\|\cdot\| = \|\cdot\|_{N_h-1}$ and $\|\cdot\|_0 = (Q, Q)$.

4 Error analysis

In this section we add one further mesh assumption: the family $\{\mathcal{T}_h\}$ is quasi-uniform in the sense stated at the beginning of Section 2. This is the standard hypothesis under which the global inverse estimate $|\chi|_1 \lesssim h^{-1} \|\chi\|$ and the spectral bound $\sup \sigma(L_h) \lesssim h^{-2}$ hold uniformly. The structural results from the previous sections did not require this stronger hypothesis.

Fix any admissible inner product $\langle \cdot, \cdot \rangle_h$. We now compare the FEM discretization based on $\langle \cdot, \cdot \rangle_h$, namely (20), and the box-method discretization based on the same inner product, namely (21), with the exact solution $u_\beta = L^{-\beta} f$. Let \widehat{L}_h denote the operator induced, in the sense of (16), by the exact form a and the exact $L^2(\mathcal{S})$ inner product on V_h , and let Π_h be the $L^2(\mathcal{S})$ -orthogonal projector onto V_h . Similarly, we write \widetilde{L}_h for the operator induced by a_h and the exact $L^2(\mathcal{S})$ inner product. Thus

$$\widehat{u}_{\beta,h} = \widehat{L}_h^{-\beta} \Pi_h f, \quad \widetilde{u}_{\beta,h} = \widetilde{L}_h^{-\beta} \Pi_h f, \quad \bar{u}_{\beta,h} = L_h^{-\beta} \Lambda_h f. \quad (33)$$

The first approximation is the classical FEM discretization; the second incorporates the quadrature error in the bilinear form while retaining the exact $L^2(\mathcal{S})$ projector; and the third further accounts for the change of inner product. The next lemma records the $L^2(\mathcal{S})$ estimate for the first of these perturbation steps; its proof is given in Appendix A.

Lemma 4.1. *Given an admissible bilinear form. Let $\widehat{u}_h = \widehat{L}_h^{-1} \Pi_h f$ and $\widetilde{u}_h = \widetilde{L}_h^{-1} \Pi_h f$. Then*

$$\|\widehat{u}_h - \widetilde{u}_h\| \lesssim h^2 \|f\|. \quad (34)$$

for sufficiently small h .

The next inverse estimate for discrete fractional norms is used repeatedly in the perturbation arguments. Its proof follows the same spectral argument as [22, Lemma 2.2]; the only point to verify in the present setting is that the spectrum of L_h remains uniformly contained in $[c, Ch^{-2}]$.

Proposition 4.2. *Let $r, s \in \mathbb{R}$ and define*

$$\|\chi\|_{s,h} = \|L_h^{s/2} \chi\|_h, \quad \chi \in V_h.$$

Then, uniformly for sufficiently small h ,

$$\|\chi\|_{r,h} \lesssim h^{-(r-s)^+} \|\chi\|_{s,h}, \quad \chi \in V_h, \quad (35)$$

where $(r-s)^+ = \max\{r-s, 0\}$.

Proof. It is enough to consider the case $r \geq s$. By coercivity and continuity of a_h on V_h , together with the norm equivalence $\|\cdot\|_h \simeq \|\cdot\|$, the Rayleigh quotient of L_h satisfies

$$c \leq \frac{\langle L_h \chi, \chi \rangle_h}{\|\chi\|_h^2} = \frac{a_h(\chi, \chi)}{\|\chi\|_h^2} \leq C \frac{|\chi|_1^2 + \|\chi\|^2}{\|\chi\|^2} \lesssim h^{-2}, \quad \chi \in V_h \setminus \{0\},$$

where the last step is the standard inverse estimate for piecewise affine finite elements. Hence the spectrum of L_h is contained in $[c, Ch^{-2}]$. Writing χ in an $\langle \cdot, \cdot \rangle_h$ -orthonormal eigenbasis of L_h , the estimate (35) follows exactly as in [22, Lemma 2.2] by comparing the spectral weights. \square

The next theorem states the rough-data estimate for the finite-element discretization under an arbitrary admissible inner product.

Theorem 4.3 (FEM estimate based on admissible inner products). *Given an admissible bilinear form and an admissible inner product. Let $f \in L^2(\mathcal{S})$, let $0 \leq \delta \leq 1$, and assume $2\beta > \delta$. Then, for all sufficiently small h ,*

$$\|u_\beta - \bar{u}_{\beta,h}\|_\delta \lesssim h^{\min\{2\beta-\delta, 2\}} \left(\log \frac{1}{h} \right)^{[2\beta-\delta=2, \delta \neq 0]} \|f\|. \quad (36)$$

We now explain the main ideas behind the proof of Theorem 4.3; the full details are given in Appendix A. Since no direct fractional analogue of Strang's lemma is available in our setting, the argument proceeds by a direct perturbation decomposition that separates the effects of the bilinear form and of the inner product. Recalling the definitions in (33), we write

$$\|u_\beta - \bar{u}_{h,\beta}\|_\delta \lesssim \|u_\beta - \hat{u}_{h,\beta}\|_\delta + \|\hat{u}_{h,\beta} - \tilde{u}_{h,\beta}\|_\delta + \|\tilde{u}_{h,\beta} - \bar{u}_{h,\beta}\|_\delta = E_1 + E_2 + E_3. \quad (37)$$

The term E_1 is the error of the fractional FEM discretization and is already well understood; see, e.g., [5, 11, 15]. The term E_2 measures the effect of replacing the exact bilinear form $a(\cdot, \cdot)$ by the admissible bilinear form $a_h(\cdot, \cdot)$, whereas E_3 measures the additional perturbation caused by replacing the exact L^2 inner product by $\langle \cdot, \cdot \rangle_h$.

The estimates for E_2 and E_3 are based on a resolvent representation of fractional powers. More precisely, if S is a bounded positive selfadjoint operator with spectrum contained in $[r, R] \subset (0, \infty)$, then the Dunford–Taylor functional calculus (see, e.g., [17]) yields the following representation of $S^{-\beta}$, valid for every $\beta > 0$:

$$\begin{aligned} S^{-\beta} &= \frac{\sin(\pi\beta)}{\pi} \int_r^R t^{-\beta} (t + S)^{-1} dt + \frac{R^{1-\beta}}{2\pi} \int_{-\pi}^{\pi} e^{i(1-\beta)\theta} (Re^{i\theta} - S)^{-1} d\theta \\ &\quad - \frac{r^{1-\beta}}{2\pi} \int_{-\pi}^{\pi} e^{i(1-\beta)\theta} (re^{i\theta} - S)^{-1} d\theta. \end{aligned} \quad (38)$$

While this identity follows from the Dunford–Taylor functional calculus, to the best of our knowledge it has not appeared in this explicit form. Its derivation and use in the present perturbation argument constitute one of our contributions. It allows us to reduce the comparison of fractional powers to the comparison of resolvents.

Among the three terms above, E_3 is the most delicate. The reason is that changing the inner product changes the realization of the discrete operator itself, so one must compare two different operator realizations together with their associated projections. The starting point of the analysis is the resolvent representation (38), which allows us to rewrite differences of fractional powers in terms of differences of resolvents. To exploit (38) in the estimate of E_3 , one needs a way to relate the two nonfractional discrete realizations. The key structural observation is the identity $T_h = \tilde{L}_h^{-1}\Pi_h = L_h^{-1}\Lambda_h$, that follows from Proposition 3.3. This shows that, although the two realizations differ at the fractional level, they coincide at the nonfractional level. It is precisely this identity that makes it possible to rewrite the resolvent difference in a form that can be estimated.

The contour representation (38) then reduces the problem to three contour contributions. The most delicate one is the integral over $[r, R]$, where the decay coming from $t^{-\beta}$ is exactly critical when $2\beta - \delta = 2$. To capture this case sharply, one chooses the upper contour radius dynamically, namely $R = (C + 1)h^{-2}$, where C is such that the spectra of both \tilde{L}_h and L_h lie below Ch^{-2} . This choice yields the logarithmic factor in the critical case and the optimal algebraic rate otherwise. The term E_2 is handled by the same general strategy, but is simpler because both operators are realized in the exact L^2 inner product, so no projection mismatch occurs. Combining the estimates for E_1 , E_2 , and E_3 yields (36).

The next result shows that we can improve the rate from Theorem 4.3 by requiring the data to be smooth.

Theorem 4.4 (FEM estimate based on admissible inner products under smooth data). *Given an admissible bilinear form and an admissible inner product. Let $f \in \dot{H}^\sigma$ with $0 \leq \sigma \leq 1$, let $0 \leq \delta \leq 1$, and assume $2\beta + \sigma > \delta$. Then, for all sufficiently small h ,*

$$\|u_\beta - \bar{u}_{\beta,h}\|_\delta \lesssim h^{\min\{2\beta+\sigma-\delta,2\}} \left(\log \frac{1}{h}\right)^{[2\beta+\sigma-\delta=2]} \|f\|_\sigma. \quad (39)$$

The proof is based on using the result of Theorem 4.3 to reduce the problem of estimating $\|L^{\frac{\delta}{2}}(\tilde{L}_h^{-\beta}\Pi_h - L_h^{-\beta}\Lambda_h)L^{-\frac{\sigma}{2}}g\|_{L(L^2(S))}$, for $g = L^{-\sigma/2}f$, to that of estimating $\|L_h^{\frac{\delta}{2}}(L_h^{-\beta}\Lambda_h - \tilde{L}_h^{-\beta}\Pi_h)\tilde{L}_h^{-\frac{\sigma}{2}}\Pi_h g\|_{L(L^2(S))}$. Then, we repeat the same strategy as in the proof of Theorem 4.3. The full proof is in Appendix A.

Finally, we return to the box-method discretization. Relative to the finite-element scheme, the only additional change is the replacement of Λ_h by P_h , that is, the use of control-volume averaging in the load term.

Lemma 4.5. *Let $0 \leq \sigma \leq 1$. Then, for every $f \in \dot{H}^\sigma$ and every $\chi \in V_h$,*

$$|(f, \chi - Q\chi)| \lesssim h^{1+\sigma} \|f\|_\sigma |\chi|_1. \quad (40)$$

Proof. For $\sigma = 0$, the estimate follows from

$\|\chi - Q\chi\| \lesssim h|\chi|_1$. For $\sigma = 1$, it is the standard barycentric lumped-mass quadrature estimate on shape-regular simplicial meshes, $|(f, \chi - Q\chi)| \lesssim h^2 |f|_1 |\chi|_1$; see, for example, [27, Chapter 4]. Interpolation between the endpoint estimates yields (40) for all $0 \leq \sigma \leq 1$. \square

Theorem 4.6 (box-method estimate). *Assume the hypotheses of Theorem 4.4. Let $u_{\beta,h} = L_h^{-\beta}P_h f$ be the box-method discretization from Definition 3.1. Then, for all sufficiently small h ,*

$$\|u_\beta - u_{\beta,h}\|_\delta \lesssim h^{\min\{2\beta+\sigma-\delta,1+\sigma\}} \left(\log \frac{1}{h}\right)^{[2\beta+\sigma-\delta=2]} \|f\|_\sigma. \quad (41)$$

The idea of the proof is as follows. We start observing that

$$u_\beta - u_{\beta,h} = (u_\beta - \bar{u}_{\beta,h}) + (\bar{u}_{\beta,h} - u_{\beta,h}).$$

The first term is estimated by Theorem 4.4, so it remains to bound the second term, which isolates the effect of the box-method load discretization. Indeed,

$$\bar{u}_{\beta,h} - u_{\beta,h} = L_h^{-\beta}(\Lambda_h - P_h)f, \quad \langle (\Lambda_h - P_h)f, \chi \rangle_h = (f, \chi - Q\chi).$$

Thus the difference comes entirely from replacing the exact load functional by its control-volume counterpart. Lemma 4.5 gives the basic estimate

$$|\langle (\Lambda_h - P_h)f, \chi \rangle_h| \lesssim h^{1+\sigma} \|f\|_\sigma |\chi|_1 \lesssim h^{1+\sigma} \|f\|_\sigma \left\| L_h^{1/2} \chi \right\|_h.$$

One then combines this bound with the mapping properties of $L_h^{-\beta}$, using the same duality argument as in the rough-data case together with Proposition 4.2. This yields

$$\|\bar{u}_{\beta,h} - u_{\beta,h}\|_\delta \lesssim h^{\min\{2\beta+\sigma-\delta, 1+\sigma\}} \|f\|_\sigma.$$

Finally, combining this estimate with Theorem 4.4 gives (41). Appendix A contains the full duality argument, including the treatment of the critical logarithmic case.

Theorem 4.6 shows the expected $h^{1+\sigma}$ saturation caused by replacing the exact load functional $\chi \mapsto (f, \chi)$ with the control-volume functional $\chi \mapsto (f, Q\chi)$. For the purposes of this paper, the main point is that this is precisely the natural accuracy barrier of the box-method load approximation, and that the choice of admissible inner product does not change the resulting convergence order.

To pass from the discrete fractional operators analyzed above to fully implementable methods, we allow for an additional exponentially convergent rational approximation of the map $\lambda \mapsto \lambda^{-\beta}$. This covers, e.g., the rational approximations of [3, 4] and the quadrature-based constructions of [5].

Assumption 4.7. For each sufficiently small h and each $m \in \mathbb{N}$, let Q_m^β be a rational function defined on a neighborhood of $\sigma(\tilde{L}_h) \cup \sigma(L_h)$, and assume that, for every $0 \leq \delta \leq 1$,

$$\sup_{\lambda \in \sigma(\tilde{L}_h) \cup \sigma(L_h)} \lambda^{\delta/2} |\lambda^{-\beta} - Q_m^\beta(\lambda)| \leq \rho_\delta(h) e^{-Cg(m)}, \quad (42)$$

where $C > 0$ is independent of h and m , the function $g : \mathbb{N} \rightarrow (0, \infty)$ satisfies $g(m) \rightarrow \infty$ as $m \rightarrow \infty$, and $\rho_\delta(h)$ is a nonnegative rational function of h .

We define the fully implementable approximations

$$\bar{u}_{\beta,h}^{(m)} := Q_m^\beta(L_h)\Lambda_h f, \quad u_{\beta,h}^{(m)} := Q_m^\beta(L_h)P_h f.$$

Corollary 4.8. *Suppose that Q_m^β satisfies Assumption 4.7 and let $0 \leq \delta \leq 1$. Then the rational approximations above converge exponentially fast to the corresponding exact discrete fractional solutions. More precisely,*

$$\|\bar{u}_{\beta,h} - \bar{u}_{\beta,h}^{(m)}\|_{\delta,h} \lesssim \rho_\delta(h) e^{-Cg(m)} \|f\|, \quad (43)$$

and

$$\|u_{\beta,h} - u_{\beta,h}^{(m)}\|_{\delta,h} \lesssim \rho_\delta(h) e^{-Cg(m)} \|f\|. \quad (44)$$

Consequently, combining (43) with Theorem 4.3, we obtain

$$\|u_\beta - \bar{u}_{\beta,h}^{(m)}\|_\delta \lesssim h^{\min\{2\beta-\delta, 2\}} \left(\log \frac{1}{h} \right)^{[2\beta-\delta=2, \delta \neq 0]} \|f\| + \rho_\delta(h) e^{-Cg(m)} \|f\|. \quad (45)$$

Likewise, combining (44) with Theorem 4.6, we obtain

$$\|u_\beta - u_{\beta,h}^{(m)}\|_\delta \lesssim h^{\min\{2\beta+\sigma-\delta, 1+\sigma\}} \left(\log \frac{1}{h}\right)^{[2\beta+\sigma-\delta=2]} \|f\|_\sigma + \rho_\delta(h) e^{-Cg(m)} \|f\|_\sigma. \quad (46)$$

In particular, if $m = m(h)$ is chosen so that the exponential term is of the same order as the corresponding spatial discretization error, then the fully implementable approximation has the same asymptotic convergence rate as the exact discrete method.

Proof. Observe that $\|\bar{u}_{\beta,h} - \bar{u}_{\beta,h}^{(m)}\|_{\delta,h} = \|L_h^{\delta/2} (L_h^{-\beta} - Q_m^\beta(L_h)) \Lambda_h f\|_h$. Hence, by the spectral theorem,

$$\|\bar{u}_{\beta,h} - \bar{u}_{\beta,h}^{(m)}\|_{\delta,h} \leq \sup_{\lambda \in \sigma(L_h)} \lambda^{\delta/2} |\lambda^{-\beta} - Q_m^\beta(\lambda)| \|\Lambda_h f\|_h.$$

Using Assumption 4.7 and the uniform boundedness of Λ_h , we obtain (43). The estimate (44) follows in the same way, using the uniform boundedness of P_h . The bounds (45) and (46) then follow immediately from the triangle inequality together with Theorems 4.3 and 4.6. \square

5 Numerical experiments

In this section, we compare our theoretical findings with numerical results. In all experiments, we take $L = -\Delta + I$, so that $A = I$ and $\kappa \equiv 1$. The one-dimensional experiments were implemented in `FEniCSx`, with the number of degrees of freedom (DOFs) given by $\{2^k + 1\}_{k=3,\dots,9}$. In our two-dimensional example, we used the `fmesh` package in `R`, together with our own implementation of the dual mesh, to carry out the experiment using an overkill solution. The main advantage of our implementation is that it constructs a matrix that allows us to assemble the load vector at each step using the same load vector employed in the overkill solution. In this last case, the DOFs range over $\{(2^k + 1)^2\}_{k=3,\dots,7}$ for the approximations, and we construct the overkill solution using order $(2^8 + 1)^2$. Fractional powers of the discrete operators were approximated using the sinc-quadrature method of [5]. In all cases, we report the error in $L^2(\mathcal{S})$; that is, we assume that $\delta = 0$. Further implementation details are available in the accompanying repository [1].

5.1 Indicator load in one dimension

We first consider $\mathcal{S} = [0, 1]$ with homogeneous Dirichlet boundary conditions and right-hand side $f = \mathbb{1}_{[0,1/2]}$. Then $f \in \dot{H}^\gamma$ for every $\gamma < 1/2$, whereas $f \notin \dot{H}^\gamma$ for $\gamma \geq 1/2$. Moreover, on a uniform one-dimensional mesh, one has $(f, \phi_z) = (f, Q\phi_z)$ for every nodal basis function ϕ_z . Therefore, the FEM and box-method error predictions coincide, and both yield the rate $\min\{2\beta + 1/2, 2\}$. The exact solution u_β is represented by the eigenbasis expansion

$$u_\beta(x) = \sum_{n=1}^{\infty} \frac{2(1 - \cos(n\pi/2))}{n\pi((n\pi)^2 + 1)^\beta} \sin(n\pi x).$$

In the computations, the reference solution was approximated by truncating this series after 8000 terms, i.e., using the sum over the terms $n = 1, \dots, 8000$. The truncation level was chosen sufficiently large so that the truncation error is negligible compared with the discretization error and thus does not affect the experimental order of convergence (EOC). Figure 3 shows that both discretizations attain the theoretical order of convergence (TOC) predicted by Corollary 4.8. The coincidence between the finite-element and box-method curves is not accidental: in one space dimension on a uniform mesh, the box average of the load matches the standard cellwise quadrature for this piecewise constant data. This experiment therefore isolates the dependence on β without introducing an additional load-discretization penalty.

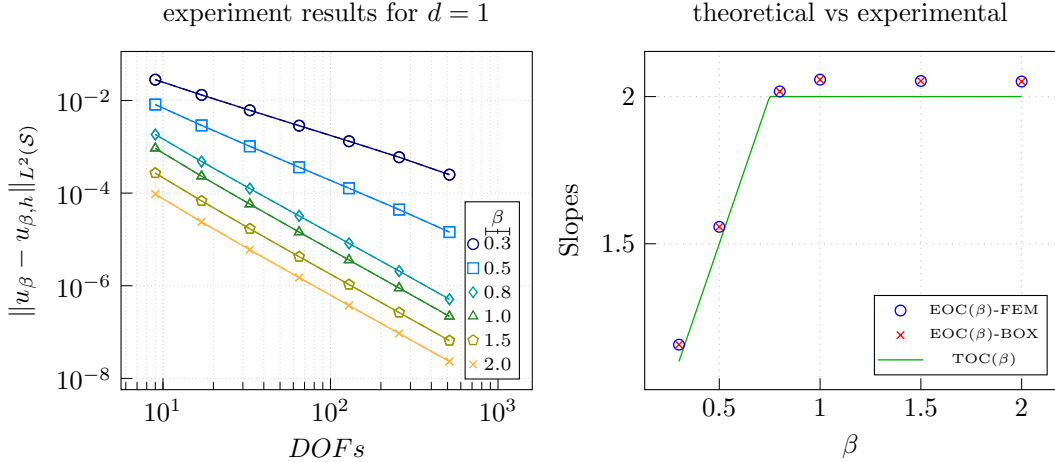


Figure 3: One-dimensional indicator load. Left: $L^2(\mathcal{S})$ error versus the number of degrees of freedom. Right: experimental orders of convergence for the finite-element and box-method discretizations compared with the theoretical slope $\min\{2\beta + 1/2, 2\}$.

5.2 A singular power load in one dimension

Our second one-dimensional test uses $f(x) = x^{-0.499}$ on $\mathcal{S} = (0, 1)$ with homogeneous Dirichlet boundary conditions. In this case, $f \in \dot{H}^\gamma$ for every $\gamma < 0.001$, whereas $f \notin \dot{H}^\gamma$ for $\gamma \geq 0.001$. The reference solution is computed by truncating the eigenfunction expansion of the exact solution u_β . More precisely, we consider

$$u_\beta(x) \approx 2 \sum_{n=1}^{2000} (n\pi)^{-2\beta} \left[\int_0^1 x^{-0.499} \sin(n\pi x) dx \right] \sin(n\pi x),$$

For $\beta = 1$, the classical box-method theory on uniform meshes predicts a rate not worse than $h^{1.5}$ for this type of singular load; see [13]. Figure 4 confirms that the observed fractional rates remain consistent with the abstract theory. In particular, the saturation visible near the larger values of β matches the fact that the spatial singularity, rather than the fractional power itself, limits the asymptotic order. As illustrated in Figure 4, the optimal convergence rate clearly exceeds 1.5 while remaining strictly below 2, in full agreement with the theoretical expectations in the case $(f, \phi_z) \neq (f, Q\phi_z)$. This example therefore confirms that the fully numerically integrated box method may fail to achieve the optimal convergence order of the full numerically integrated finite element method.

5.3 Changing inner products in two dimensions

We now consider a Neumann problem on the unit square $\mathcal{S} = [0, 1]^2$, with

$$f(x, y) = -\text{sign}\left(\left(x - \frac{1}{2}\right)\left(y - \frac{1}{2}\right)\right).$$

This load belongs to \dot{H}^γ for every $\gamma < 1/2$, and our main interest here is not the FEM/box-method comparison but the dependence on the auxiliary inner product. We therefore fix the box-method discretization and compare three admissible inner products: the exact $L^2(\mathcal{S})$ product and $\langle \cdot, \cdot \rangle_0$ and $\langle \cdot, \cdot \rangle_1$ from Proposition 3.7. Figure 5 shows that the observed slope is the same for all three choices, in agreement with the theory. The experiment thus supports the message of Sections 3 and 4: admissible inner products change the discrete fractional operator, but not the convergence order.

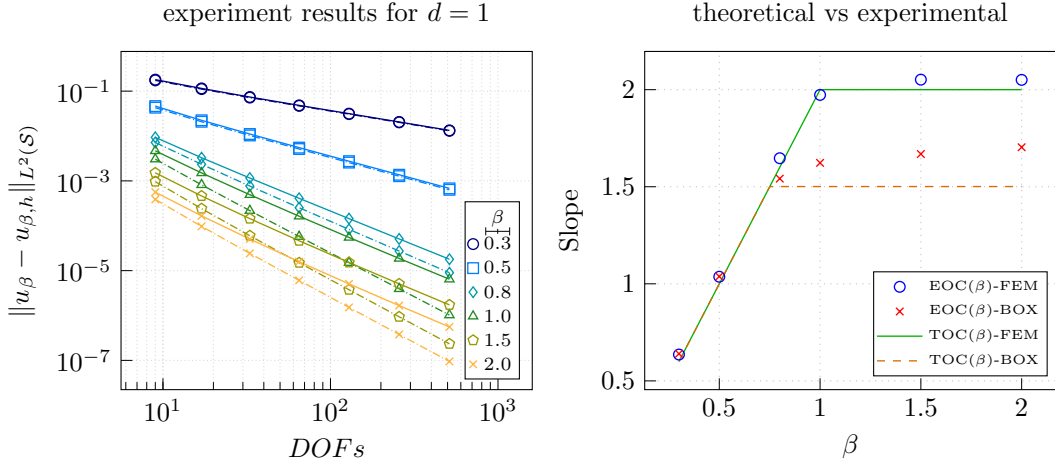


Figure 4: One-dimensional singular load $f(x) = x^{-0.499}$. Left: $L^2(\mathcal{S})$ error versus the number of degrees of freedom. Right: experimental slopes compared with the theoretical prediction.

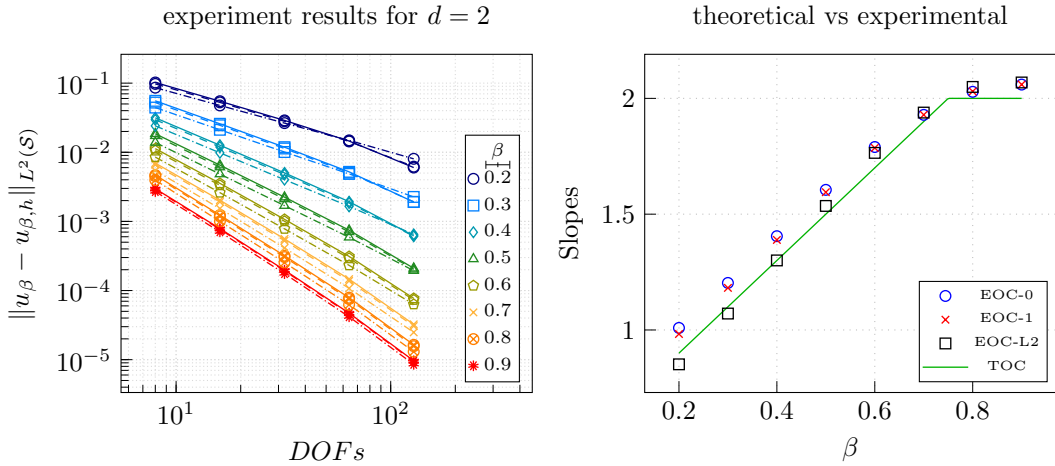


Figure 5: Two-dimensional checkerboard load. Left: $L^2(\mathcal{S})$ error versus the number of degrees of freedom for three admissible inner products. Right: experimental slopes compared with the common theoretical prediction $\min\{2\beta + 1/2, 2\}$.

6 Conclusion

We have developed a finite-dimensional framework for fractional elliptic discretization that keeps the bilinear form, the load discretization, and the inner product on the trial space separate. The analysis shows that this separation is not cosmetic. For $\beta \neq 1$, different admissible inner products genuinely lead to different discrete fractional operators, while the lumped-mass choice is singled out by an intrinsic representation in terms of the nonfractional box solution operator. Under natural second-order consistency assumptions, the finite-element discretization preserves the classical fractional FEM rate and the box-method discretization suffers only the expected loss coming from control-volume averaging of the load. The numerical experiments support both conclusions. Finally, we stress that the present work was strongly motivated by the need to explain the success of the so-called SPDE approach in statistics, and that it provides the analytical basis for investigating mass-lumping techniques in that setting. More broadly, the framework developed here also opens several directions for future work, including the analysis of discretizations of fractional parabolic problems, such as fractional heat equations, and

their associated stochastic partial differential equations, which are of interest in spatio-temporal statistics.

Acknowledgments: The authors declare that they have no conflict of interest.

A Auxiliary proofs and technical estimates

This supplement contains the proofs and technical estimates used in the main text. We use the notation of the main text. In particular, $d \in \{1, 2, 3\}$, $\mathcal{S} \subset \mathbb{R}^d$ is a bounded convex interval, polygon, or polyhedron as appropriate, $\{\mathcal{T}_h\}$ is a conforming shape-regular simplicial mesh family, V_h is the conforming P_1 trial space, $V_{0,h}$ is the space of piecewise constants on the barycentric dual mesh, and the box transfer operator is

$$Q\chi = \sum_{z \in \mathcal{Z}_h^{\text{act}}} \chi(z) \mathbb{1}_{b_z}.$$

The nonfractional box method is the standard vertex-centered finite-volume scheme on the dual cells b_z ; classical references include [2, 8, 21]. Its balance equations were recalled in Section 2 from the main text. We also use the fractional Hilbert scale $\dot{H}^s(\mathcal{S})$ associated with the positive selfadjoint operator $L = -\text{div}(A\nabla) + \kappa^2$, with $\dot{H}^s(\mathcal{S}) = D(L^{s/2})$ for $s \geq 0$ and the completion/duality definition for $s < 0$. The contour formulas used later are standard consequences of the holomorphic functional calculus for positive sectorial operators; see, for example, [5, 17]. For Hilbert spaces X and Y , we write $L(X, Y)$ for the space of bounded linear operators from X to Y , and abbreviate $L(X, X)$ by $L(X)$. The corresponding operator norm is denoted by $\|\cdot\|_{L(X,Y)}$, and by $\|\cdot\|_{L(X)}$ when $X = Y$.

B Proofs from Section 2

For a simplex $K \in \mathcal{T}_h$ and a vertex $z \in \mathcal{Z}(K)$, let

$$\Gamma_{z,K} := \partial b_z \cap K.$$

This is the part of the control-volume boundary contained in K . When $d = 2$, $\Gamma_{z,K}$ is the broken line joining the two edge midpoints adjacent to z to the barycenter of K . When $d = 3$, $\Gamma_{z,K}$ is the union of three quadrilateral faces.

Lemma B.1. *Let $K \in \mathcal{T}_h$, let $z \in \mathcal{Z}(K)$, and let ϕ_z denote the local nodal basis function associated with z . For every constant vector $p \in \mathbb{R}^d$,*

$$- \int_{\Gamma_{z,K}} p \cdot \eta_{z,K} ds = \int_K p \cdot \nabla \phi_z dx = |K| p \cdot \nabla \phi_z. \quad (47)$$

Here $\eta_{z,K}$ is the outward unit normal to b_z restricted to $\Gamma_{z,K}$.

Proof. Both sides of (47) are covariant under affine changes of variables. Indeed, if $F(\hat{x}) = B\hat{x} + b$ maps the reference simplex \hat{K} to K , then

$$\nabla \phi_z = B^{-T} \nabla \hat{\phi}_z, \quad |K| = |\det B| |\hat{K}|,$$

and the surface integral transforms by the standard affine change-of-variables formula. Therefore it is enough to verify (47) on the reference simplex.

For $d = 1$, $\widehat{K} = (0, 1)$. For the left endpoint, $\Gamma_{0, \widehat{K}} = \{1/2\}$ and the outward normal equals $+1$, while $\widehat{\phi}_0(x) = 1 - x$. Hence

$$- \int_{\Gamma_{0, \widehat{K}}} p \eta ds = -p = \int_0^1 p \widehat{\phi}'_0(x) dx.$$

The right endpoint is identical.

For $d = 2$, take $\widehat{K} = \text{conv}\{(0, 0), (1, 0), (0, 1)\}$. Here $\text{conv}\{(0, 0), (1, 0), (0, 1)\}$ denotes the convex hull of the three vertices, i.e., the reference triangle with corners $(0, 0)$, $(1, 0)$, and $(0, 1)$. For the vertex $z_0 = (0, 0)$, the boundary $\Gamma_{z_0, \widehat{K}}$ consists of the two segments

$$[(1/2, 0), (1/3, 1/3)] \quad \text{and} \quad [(1/3, 1/3), (0, 1/2)].$$

The corresponding outward normal vectors integrated along the segments add up to $(1/2, 1/2)$. Since $\widehat{\phi}_{z_0}(x, y) = 1 - x - y$ and $|\widehat{K}| = 1/2$, we obtain

$$- \int_{\Gamma_{z_0, \widehat{K}}} p \cdot \eta ds = -p \cdot (1/2, 1/2) = |\widehat{K}| p \cdot \nabla \widehat{\phi}_{z_0}.$$

The remaining vertices follow by symmetry.

For $d = 3$, take $\widehat{K} = \text{conv}\{(0, 0, 0), (1, 0, 0), (0, 1, 0), (0, 0, 1)\}$. For the vertex $z_0 = (0, 0, 0)$, the set $\Gamma_{z_0, \widehat{K}}$ is the union of three quadrilaterals. The area vectors of those quadrilaterals are

$$\left(\frac{1}{12}, \frac{1}{24}, \frac{1}{24}\right), \quad \left(\frac{1}{24}, \frac{1}{12}, \frac{1}{24}\right), \quad \left(\frac{1}{24}, \frac{1}{24}, \frac{1}{12}\right),$$

so that

$$\int_{\Gamma_{z_0, \widehat{K}}} \eta ds = \left(\frac{1}{6}, \frac{1}{6}, \frac{1}{6}\right).$$

Since $\widehat{\phi}_{z_0}(x, y, z) = 1 - x - y - z$ and $|\widehat{K}| = 1/6$, we conclude that

$$- \int_{\Gamma_{z_0, \widehat{K}}} p \cdot \eta ds = -p \cdot \left(\frac{1}{6}, \frac{1}{6}, \frac{1}{6}\right) = |\widehat{K}| p \cdot \nabla \widehat{\phi}_{z_0}.$$

Again the other vertices are obtained by symmetry. □

The lemma implies the exactness of the box diffusion term for cellwise constant coefficients. Related nonfractional flux computations may also be found in [23].

Proof of Lemma 2.1 from the main text. Since $\nabla \chi$ is constant on K , Lemma B.1 gives

$$- \sum_{z \in \mathcal{Z}(K)} \psi(z) \int_{\Gamma_{z, K}} B \nabla \chi \cdot \eta_{z, K} ds = |K| \sum_{z \in \mathcal{Z}(K)} \psi(z) B \nabla \chi \cdot \nabla \phi_z.$$

Because $\psi = \sum_{z \in \mathcal{Z}(K)} \psi(z) \phi_z$ on K , the right-hand side equals

$$|K| B \nabla \chi \cdot \nabla \psi = \int_K B \nabla \chi \cdot \nabla \psi dx.$$

Therefore, we obtain

$$- \sum_{z \in \mathcal{Z}(K)} \psi(z) \int_{\Gamma_{z, K}} B \nabla \chi \cdot \eta_{z, K} ds = \int_K B \nabla \chi \cdot \nabla \psi dx. \quad (48)$$

The result thus follows by summing (48) over all elements and adding the reaction term. □

Proof of Lemma 2.2 from the main text. The definition of the bilinear form $a_h^{A_h}$ uses the piecewise constant function A_h determined by the cell averages $A_K := A_h|_K$ and therefore falls exactly under Lemma 2.1 from the main text on every element. Summing (48) over the mesh yields

$$- \sum_{z \in \mathcal{Z}_h^{\text{act}}} \psi(z) \int_{\partial b_z} A_K \nabla \chi \cdot \eta \, ds = \sum_{K \in \mathcal{T}_h} \int_K A_K \nabla \chi \cdot \nabla \psi \, dx.$$

Since $\nabla \chi|_K$ and $\nabla \psi|_K$ are constant on each element and A_K is the mean value of A on K ,

$$\int_K A_K \nabla \chi \cdot \nabla \psi \, dx = \int_K A \nabla \chi \cdot \nabla \psi \, dx.$$

Adding the reaction term gives

$$a_h^{A_h}(\chi, \psi) = \int_S A \nabla \chi \cdot \nabla \psi \, dx + (\kappa_Q \chi, \kappa_Q \psi),$$

which is symmetric. □

Proof of Theorem 2.3 from the main text. By Lemma 2.2, we have that

$$a_h^{A_h}(\chi, \psi) = \int_S A \nabla \chi \cdot \nabla \psi \, dx + (\kappa_Q \chi, \kappa_Q \psi). \quad (49)$$

In particular,

$$a_h^{A_h}(\chi, \chi) \geq \alpha |\chi|_1^2 + \kappa_0^2 \|\kappa_Q \chi\|^2, \quad (50)$$

where $\alpha > 0$ is the ellipticity constant of A and $\kappa_0 = \text{ess inf}_{x \in S} \kappa(x) > 0$.

The piecewise-constant norm induced by Q is uniformly equivalent to the L^2 norm on V_h :

$$c_Q \|\chi\|^2 \leq \|\kappa_Q \chi\|^2 \leq C_Q \|\chi\|^2 \quad \forall \chi \in V_h, \quad (51)$$

with constants depending only on the shape-regularity of the mesh family; see, for example, [9, 27]. Consequently,

$$a_h^{A_h}(\chi, \chi) \geq c \left(|\chi|_{H^1(S)}^2 + \|\chi\|^2 \right) \quad (52)$$

for a constant $c > 0$ independent of h .

We now compare a_h^A and $a_h^{A_h}$. Fix $\chi, \psi \in V_h$. On each element K , set

$$\bar{\psi}_K := \frac{1}{d+1} \sum_{z \in \mathcal{Z}(K)} \psi(z).$$

As in the previous proof, let $A_K := A_h|_K$. Since the sum of the local fluxes over all control-volume interfaces in K vanishes, we may subtract the constant $\bar{\psi}_K$ from the nodal values and write

$$a_h^A(\chi, \psi) - a_h^{A_h}(\chi, \psi) = - \sum_{K \in \mathcal{T}_h} \sum_{z \in \mathcal{Z}(K)} (\psi(z) - \bar{\psi}_K) \int_{\Gamma_{z,K}} (A - A_K) \nabla \chi \cdot \eta_{z,K} \, ds.$$

For affine ψ on K we have $|\psi(z) - \bar{\psi}_K| \leq Ch_K |\nabla \psi|_{L^2(K)}$, while

$$\|A - A_K\|_{L^\infty(K)} \leq Ch_K \|A\|_{W^{1,\infty}(K)}, \quad \mathcal{H}^{d-1}(\Gamma_{z,K}) \leq Ch_K^{d-1},$$

where $\mathcal{H}^{d-1}(\Gamma_{z,K})$ denotes the $(d-1)$ -dimensional Hausdorff measure of $\Gamma_{z,K}$, that is, its length when $d = 2$ and its surface area when $d = 3$. Therefore

$$\left| a_h^A(\chi, \psi) - a_h^{A_h}(\chi, \psi) \right| \leq C \sum_{K \in \mathcal{T}_h} h_K^{d+1} |\nabla \chi|_{L^2(K)} |\nabla \psi|_{L^2(K)}$$

$$\leq Ch \sum_{K \in \mathcal{T}_h} |K| |\nabla \chi|_{L^2(K)} |\nabla \psi|_{L^2(K)} \leq Ch |\chi|_{H^1(\mathcal{S})} |\psi|_{H^1(\mathcal{S})}.$$

Combining this perturbation bound with (52) yields

$$a_h^A(\chi, \chi) \geq a_h^{A_h}(\chi, \chi) - Ch |\chi|_{H^1(\mathcal{S})}^2 \geq \frac{c}{2} \|\chi\|_{H^1(\mathcal{S})}^2$$

for all sufficiently small h . This proves the theorem. \square

Proof of Proposition 2.8 from the main text. Let P_h and Λ_h be defined by

$$\langle P_h f, \chi \rangle_h = (f, Q\chi), \quad \langle \Lambda_h f, \chi \rangle_h = (f, \chi).$$

Item 1. For $f \in L^2(\mathcal{S})$ and $\chi \in V_h$,

$$\langle P_h f, \chi \rangle_h = (f, Q\chi) = (\Pi_{0,h} f, Q\chi) = \langle P_h \Pi_{0,h} f, \chi \rangle_h.$$

Hence $P_h = P_h \Pi_{0,h}$.

Item 2. If $\|Q\chi\| \leq C \|\chi\|_h$, then

$$|\langle P_h f, \chi \rangle_h| = |(f, Q\chi)| \leq \|f\| \|Q\chi\| \leq C \|f\| \|\chi\|_h.$$

Choosing $\chi = P_h f$ yields $\|P_h f\|_h \leq C \|f\|$.

Item 3. Using the expansion

$$Q\chi = \sum_{z \in \mathcal{Z}_h^{\text{act}}} \chi(z) \mathbb{1}_{b_z}, \quad \Pi_{0,h} f = \sum_{z \in \mathcal{Z}_h^{\text{act}}} (\Pi_{0,h} f|_{b_z}) \mathbb{1}_{b_z},$$

we obtain

$$\langle P_h f, \chi \rangle_h = (\Pi_{0,h} f, Q\chi) = \sum_{z \in \mathcal{Z}_h^{\text{act}}} \Pi_{0,h} f|_{b_z} \chi(z) |b_z|.$$

Hence $P_h f = 0$ if and only if $\Pi_{0,h} f|_{b_z} = 0$ for every active vertex z . To show surjectivity, fix $\alpha \in V_h$ and set

$$f_\alpha := \sum_{z \in \mathcal{Z}_h^{\text{act}}} \frac{\langle \alpha, \phi_z \rangle_h}{|b_z|} \mathbb{1}_{b_z}.$$

Then for every $\chi \in V_h$,

$$(f_\alpha, Q\chi) = \sum_{z \in \mathcal{Z}_h^{\text{act}}} \frac{\langle \alpha, \phi_z \rangle_h}{|b_z|} (\mathbb{1}_{b_z}, Q\chi) = \sum_{z \in \mathcal{Z}_h^{\text{act}}} \langle \alpha, \phi_z \rangle_h \chi(z) = \langle \alpha, \chi \rangle_h.$$

Thus $P_h f_\alpha = \alpha$.

Item 4. For $f, g \in L^2(\mathcal{S})$, $(f, P_h g) = \langle \Lambda_h f, P_h g \rangle_h = (Q\Lambda_h f, g)$. Therefore we have $P_h^* = Q\Lambda_h$ as an operator on $L^2(\mathcal{S})$. \square

Proof of Corollary 2.9 from the main text. Assume first that $\langle \chi, \psi \rangle_h = (\chi, Q\psi)$ for all $\chi, \psi \in V_h$. Then

$$\langle P_h \chi, \psi \rangle_h = (\chi, Q\psi) = \langle \chi, \psi \rangle_h \quad \forall \chi, \psi \in V_h,$$

so $P_h \chi = \chi$ for every $\chi \in V_h$. Since $\text{Ran}(P_h) = V_h$ by Proposition 2.8, it follows that P_h is a projection.

Conversely, suppose that P_h is a projection. Since $\text{Ran}(P_h) = V_h$, we have $P_h \chi = \chi$ for every $\chi \in V_h$. Then

$$\langle \chi, \psi \rangle_h = \langle P_h \chi, \psi \rangle_h = (\chi, Q\psi) \quad \forall \chi, \psi \in V_h.$$

Thus the inner product must be $(\cdot, Q\cdot)$. Finally, Proposition 2.8 gives $P_h^* = Q\Lambda_h$, whose range is contained in $V_{0,h}$. Since $\text{Ran}(P_h) = V_h$, the operator P_h cannot be self-adjoint on $L^2(\mathcal{S})$ and therefore is never an orthogonal projection. \square

C Proofs of the error estimates

In this section, we additionally assume quasi-uniformity of the mesh family, as in Section 4 from the main text. This is the hypothesis that allows the inverse estimate and the global spectral bound to be written in terms of the single mesh parameter h .

We let \widehat{L}_h denote the operator induced by the exact bilinear form $a(\cdot, \cdot)$ relative to the exact L^2 inner product, while \widetilde{L}_h denotes the operator induced by $a_h(\cdot, \cdot)$ relative to the exact L^2 inner product, and L_h denotes the operator induced by $a_h(\cdot, \cdot)$ relative to the admissible inner product $\langle \cdot, \cdot \rangle_h$. Thus

$$\widehat{u}_{\beta,h} = \widehat{L}_h^{-\beta} \Pi_h f, \quad \widetilde{u}_{\beta,h} = \widetilde{L}_h^{-\beta} \Pi_h f, \quad \bar{u}_{\beta,h} = L_h^{-\beta} \Lambda_h f.$$

Proof of Lemma 4.1 from the main text. Set $e_h = \widehat{u}_h - \widetilde{u}_h$. Since $a(\widehat{u}_h, \chi) = (f, \chi) = a_h(\widetilde{u}_h, \chi)$ for all $\chi \in V_h$, we have

$$\begin{aligned} a(e_h, \chi) &= a(\widehat{u}_h - \widetilde{u}_h, \chi) = a(\widehat{u}_h, \chi) - a(\widetilde{u}_h, \chi) \\ &= (f, \chi) - a(\widetilde{u}_h, \chi) = a_h(\widetilde{u}_h, \chi) - a(\widetilde{u}_h, \chi) = (a_h - a)(\widetilde{u}_h, \chi). \end{aligned} \quad (53)$$

Taking $\chi = e_h$ and using Definition 2.5 from the main text together with the coercivity of a gives

$$\|e_h\|_{H^1(S)}^2 \lesssim a(e_h, e_h) = (a_h - a)(\widetilde{u}_h, e_h) \lesssim h^2 |\widetilde{u}_h|_1 |e_h|_1 \lesssim h^2 \|\widetilde{u}_h\|_{H^1(S)} \|e_h\|_{H^1(S)}.$$

Hence

$$\|e_h\|_{H^1(S)} \lesssim h^2 \|\widetilde{u}_h\|_{H^1(S)}. \quad (54)$$

Next, by coercivity of a_h on V_h for sufficiently small h (see Remark 2.6 from the main text) and the discrete equation for \widetilde{u}_h ,

$$\|\widetilde{u}_h\|_{H^1(S)}^2 \lesssim a_h(\widetilde{u}_h, \widetilde{u}_h) = (f, \widetilde{u}_h) \leq \|f\| \|\widetilde{u}_h\| \leq \|f\| \|\widetilde{u}_h\|_{H^1(S)}.$$

Therefore

$$\|\widetilde{u}_h\|_{H^1(S)} \lesssim \|f\|. \quad (55)$$

Combining (54) and (55), we obtain $\|e_h\|_{H^1(S)} \lesssim h^2 \|f\|$. Further, since $\|e_h\| \leq \|e_h\|_{H^1(S)}$, it follows that $\|e_h\| \lesssim h^2 \|f\|$, which proves (34) from the main text. \square

Proof of Theorem 4.3 from the main text. We decompose the error as

$$u_\beta - \bar{u}_{\beta,h} = (u_\beta - \widehat{u}_{\beta,h}) + (\widehat{u}_{\beta,h} - \widetilde{u}_{\beta,h}) + (\widetilde{u}_{\beta,h} - \bar{u}_{\beta,h}) =: E_1 + E_2 + E_3. \quad (56)$$

The term E_1 is the classical finite element error for fractional powers. Thus

$$\|E_1\|_\delta \lesssim h^{\min\{2\beta-\delta, 2\}} \left(\log \frac{1}{h} \right)^{[2\beta-\delta=2, \delta>0]} \|f\|; \quad (57)$$

see [5, 11, 15].

We next estimate E_3 , which is the most delicate term. The key observation is that

$$\widetilde{L}_h^{-1} \Pi_h = L_h^{-1} \Lambda_h =: T_h, \quad (58)$$

because both sides are the discrete solution operator for the nonfractional problem associated with the bilinear form a_h .

Let $\tilde{\lambda}_{1,h}$ and $\lambda_{1,h}$ denote the smallest eigenvalues of \widetilde{L}_h and L_h , respectively. Since both operators are positive selfadjoint, their smallest eigenvalues admit the Rayleigh quotient characterizations

$$\tilde{\lambda}_{1,h} = \inf_{\chi \in V_h \setminus \{0\}} \frac{a_h(\chi, \chi)}{\|\chi\|^2}, \quad \lambda_{1,h} = \inf_{\chi \in V_h \setminus \{0\}} \frac{a_h(\chi, \chi)}{\|\chi\|_h^2}.$$

By Remark 2.6 and Definition 2.4(ii), both quotients are bounded below by a positive constant independent of h . Hence there exists $c_0 > 0$, independent of h , such that

$$\tilde{\lambda}_{1,h} \geq c_0, \quad \lambda_{1,h} \geq c_0.$$

We therefore fix once and for all

$$0 < r < \frac{c_0}{2},$$

so that $r < \min\{\tilde{\lambda}_{1,h}, \lambda_{1,h}\}$ for all sufficiently small h . In particular, r is independent of h .

Next, let $\tilde{\lambda}_{N_h,h}$ and $\lambda_{N_h,h}$ denote the largest eigenvalues of \tilde{L}_h and L_h . By the global inverse estimate, there exists $C > 0$, independent of h , such that

$$\max\{\tilde{\lambda}_{N_h,h}, \lambda_{N_h,h}\} \leq Ch^{-2}.$$

We then set

$$R = (C + 1)h^{-2}.$$

We now recall the contour representation of the fractional power. Let A be a finite-dimensional positive selfadjoint operator with $\sigma(A) \subset [r, R]$. For any contour Γ encircling $\sigma(A)$ and avoiding the origin, the Dunford–Taylor formula gives

$$A^{-\beta} = \frac{1}{2\pi i} \int_{\Gamma} z^{-\beta} (zI - A)^{-1} dz; \quad (59)$$

see [17]. We apply this formula to the keyhole contour

$$\Gamma_{\omega} = \Gamma_{1,\omega} \cup \Gamma_{2,\omega} \cup \Gamma_{3,\omega} \cup \Gamma_{4,\omega}, \quad 0 < \omega < \pi,$$

where

$$\begin{aligned} \Gamma_{1,\omega} &= \{z(t) = te^{i\omega} : t \in [\overleftarrow{r}, \overleftarrow{R}]\}, & \Gamma_{2,\omega} &= \{z(\theta) = Re^{i\theta} : \theta \in [\overleftarrow{-\omega}, \overleftarrow{\omega}]\}, \\ \Gamma_{3,\omega} &= \{z(t) = te^{-i\omega} : t \in [\overrightarrow{r}, \overrightarrow{R}]\}, & \Gamma_{4,\omega} &= \{z(\theta) = re^{i\theta} : \theta \in [\overrightarrow{-\omega}, \overrightarrow{\omega}]\}. \end{aligned}$$

Writing the contour integral explicitly, we obtain

$$\begin{aligned} 2\pi i A^{-\beta} &= e^{(1-\beta)i\omega} \int_R^r t^{-\beta} (te^{i\omega} - A)^{-1} dt + e^{(\beta-1)i\omega} \int_r^R t^{-\beta} (te^{-i\omega} - A)^{-1} dt \\ &\quad + iR^{1-\beta} \int_{-\omega}^{\omega} e^{i(1-\beta)\theta} (Re^{i\theta} - A)^{-1} d\theta - ir^{1-\beta} \int_{-\omega}^{\omega} e^{i(1-\beta)\theta} (re^{i\theta} - A)^{-1} d\theta. \end{aligned} \quad (60)$$

Passing to the limit $\omega \uparrow \pi$, we arrive at

$$\begin{aligned} A^{-\beta} &= \frac{\sin(\pi\beta)}{\pi} \int_r^R t^{-\beta} (t + A)^{-1} dt + \frac{R^{1-\beta}}{2\pi} \int_{-\pi}^{\pi} e^{i(1-\beta)\theta} (Re^{i\theta} - A)^{-1} d\theta \\ &\quad - \frac{r^{1-\beta}}{2\pi} \int_{-\pi}^{\pi} e^{i(1-\beta)\theta} (re^{i\theta} - A)^{-1} d\theta. \end{aligned} \quad (61)$$

This formula is valid in particular for $A = \tilde{L}_h$ and $A = L_h$.

We now explain how (61) leads to an estimate for E_3 . Define

$$\mathcal{E}_h := \tilde{L}_h^{\delta/2} (\tilde{L}_h^{-\beta} \Pi_h - L_h^{-\beta} \Lambda_h) \in L(L^2(\mathcal{S})).$$

Since $E_3 = (\tilde{L}_h^{-\beta} \Pi_h - L_h^{-\beta} \Lambda_h)f$ and, for $0 \leq \delta \leq 1$, the norms $\|\cdot\|_{\delta}$ and $\|\tilde{L}_h^{\delta/2} \cdot\|$ are equivalent on V_h with constants independent of h , we have

$$\|E_3\|_{\delta} \lesssim \|\mathcal{E}_h f\| \leq \|\mathcal{E}_h\|_{L(L^2(\mathcal{S}))} \|f\|.$$

Applying (61) to $\tilde{L}_h^{-\beta}$ and $L_h^{-\beta}$, we therefore obtain

$$\begin{aligned} \|E_3\|_\delta \lesssim \|f\| & \left(\int_r^R t^{-\beta} \|\tilde{L}_h^{\delta/2} \mathcal{I}_1\|_{L(L^2(\mathcal{S}))} dt \right. \\ & + R^{1-\beta} \int_{-\pi}^\pi \|\tilde{L}_h^{\delta/2} \mathcal{I}_2\|_{L(L^2(\mathcal{S}))} d\theta \\ & \left. + r^{1-\beta} \int_{-\pi}^\pi \|\tilde{L}_h^{\delta/2} \mathcal{I}_3\|_{L(L^2(\mathcal{S}))} d\theta \right), \end{aligned} \quad (62)$$

where

$$\begin{aligned} \mathcal{I}_1 &= (t + \tilde{L}_h)^{-1} \Pi_h - (t + L_h)^{-1} \Lambda_h, \\ \mathcal{I}_2 &= (Re^{i\theta} - \tilde{L}_h)^{-1} \Pi_h - (Re^{i\theta} - L_h)^{-1} \Lambda_h, \\ \mathcal{I}_3 &= (re^{i\theta} - \tilde{L}_h)^{-1} \Pi_h - (re^{i\theta} - L_h)^{-1} \Lambda_h. \end{aligned}$$

We first estimate \mathcal{I}_1 . Using (58), we obtain

$$\begin{aligned} \mathcal{I}_1 &= (t + \tilde{L}_h)^{-1} \tilde{L}_h T_h - (t + L_h)^{-1} L_h T_h \\ &= t(t + \tilde{L}_h)^{-1} \tilde{L}_h (\tilde{L}_h^{-1} - L_h^{-1}) L_h (t + L_h)^{-1} T_h \\ &= t(t + \tilde{L}_h)^{-1} \tilde{L}_h^{1/2} \tilde{L}_h^{1/2} (\tilde{L}_h^{-1} - L_h^{-1}) L_h (t + L_h)^{-1} T_h. \end{aligned} \quad (63)$$

We claim that

$$\|\tilde{L}_h^{1/2} (\tilde{L}_h^{-1} - L_h^{-1})\|_{L(V_h)} \lesssim h^2 \|L_h^{1/2}\|_{L(V_h)}, \quad (64)$$

that is,

$$\|\tilde{L}_h^{1/2} (\tilde{L}_h^{-1} - L_h^{-1}) \psi\| \lesssim h^2 \|L_h^{1/2} \psi\|_h, \quad \psi \in V_h. \quad (65)$$

Indeed, setting

$$\xi = (\tilde{L}_h^{-1} - L_h^{-1}) \psi,$$

we have

$$\begin{aligned} \|\tilde{L}_h^{1/2} \xi\|^2 &= a_h(\xi, \xi) = (\psi, \xi) - \langle \psi, \xi \rangle_h \\ &\lesssim h^2 |\psi|_1 |\xi|_1 \lesssim h^2 a_h(\psi, \psi)^{1/2} a_h(\xi, \xi)^{1/2} \\ &= h^2 \|L_h^{1/2} \psi\|_h \|\tilde{L}_h^{1/2} \xi\|, \end{aligned}$$

which proves (65).

Combining (63) and (65), we obtain

$$\|\tilde{L}_h^{\delta/2} \mathcal{I}_1\|_{L(L^2(\mathcal{S}))} \lesssim h^2 t \|\tilde{L}_h^{\delta/2} (t + \tilde{L}_h)^{-1} \tilde{L}_h^{1/2}\|_{L(L^2(\mathcal{S}))} \|L_h^{3/2} (t + L_h)^{-1} T_h\|_{L(L^2(\mathcal{S}))}. \quad (66)$$

We now estimate the two factors by the spectral theorem. Since \tilde{L}_h is positive selfadjoint,

$$\|\tilde{L}_h^{\delta/2} (t + \tilde{L}_h)^{-1} \tilde{L}_h^{1/2}\|_{L(L^2(\mathcal{S}))} = \sup_{\lambda \in \sigma(\tilde{L}_h)} \frac{\lambda^{\frac{1}{2} + \frac{\delta}{2}}}{t + \lambda} \lesssim t^{\frac{\delta}{2} - \frac{1}{2}}. \quad (67)$$

Likewise, using $T_h = L_h^{-1} \Lambda_h$ and the uniform boundedness of Λ_h ,

$$\begin{aligned} \|L_h^{3/2} (t + L_h)^{-1} T_h\|_{L(L^2(\mathcal{S}))} &= \|L_h^{1/2} (t + L_h)^{-1} \Lambda_h\|_{L(L^2(\mathcal{S}))} \\ &\lesssim \sup_{\lambda \in \sigma(L_h)} \frac{\lambda^{1/2}}{t + \lambda} \lesssim t^{-1/2}. \end{aligned} \quad (68)$$

Substituting (67) and (68) into (66) yields

$$\|\tilde{L}_h^{\delta/2} \mathcal{I}_1\|_{L(L^2(\mathcal{S}))} \lesssim h^2 t^{\delta/2}.$$

Therefore

$$\int_r^R t^{-\beta} \|\tilde{L}_h^{\delta/2} \mathcal{I}_1\|_{L(L^2(\mathcal{S}))} dt \lesssim h^2 \int_r^R t^{-\beta+\delta/2} dt \lesssim h^{\min\{2\beta-\delta, 2\}} \left(\log \frac{1}{h}\right)^{[2\beta-\delta=2]}. \quad (69)$$

Indeed, if $2\beta - \delta \neq 2$, the integral is bounded by $R^{1-\beta+\delta/2}$, and since $R = (C+1)h^{-2}$ this gives $h^{2\beta-\delta}$ when $2\beta - \delta < 2$ and h^2 otherwise. In the critical case $2\beta - \delta = 2$, the integral equals $\log(R/r) \lesssim \log(1/h)$.

To estimate the contribution on the large circular arc, we argue as in the treatment of \mathcal{I}_1 . First,

$$\begin{aligned} \|\tilde{L}_h^{\delta/2} \mathcal{I}_2\|_{L(L^2(\mathcal{S}))} &\lesssim h^2 R \|\tilde{L}_h^{\delta/2} (Re^{i\theta} - \tilde{L}_h)^{-1} \tilde{L}_h^{1/2}\|_{L(L^2(\mathcal{S}))} \\ &\quad \|\tilde{L}_h^{3/2} (Re^{i\theta} - L_h)^{-1} T_h\|_{L(L^2(\mathcal{S}))}. \end{aligned} \quad (70)$$

We now estimate the two factors on the right-hand side by the spectral theorem. Since $\sigma(\tilde{L}_h) \subset [r, Ch^{-2}]$ and $R = (C+1)h^{-2}$, we have

$$|Re^{i\theta} - \lambda| \geq h^{-2} |(C+1)e^{i\theta} - C|, \quad \lambda \in \sigma(\tilde{L}_h).$$

Hence

$$\begin{aligned} R^{1-\beta/2} \|\tilde{L}_h^{\delta/2} (Re^{i\theta} - \tilde{L}_h)^{-1} \tilde{L}_h^{1/2}\|_{L(L^2(\mathcal{S}))} &= R^{1-\beta/2} \sup_{\lambda \in \sigma(\tilde{L}_h)} \frac{\lambda^{\frac{1}{2}+\frac{\delta}{2}}}{|Re^{i\theta} - \lambda|} \\ &\leq R^{1-\beta/2} \frac{(Ch^{-2})^{\frac{1}{2}+\frac{\delta}{2}}}{h^{-2} |(C+1)e^{i\theta} - C|} = \frac{(C+1)^{1-\beta/2} C^{\frac{1}{2}+\frac{\delta}{2}}}{|(C+1)e^{i\theta} - C|} h^{\beta-\delta-1}. \end{aligned}$$

Since

$$|(C+1)e^{i\theta} - C| \geq 1 \quad \text{for all } \theta \in [-\pi, \pi],$$

it follows that

$$R^{1-\beta/2} \|\tilde{L}_h^{\delta/2} (Re^{i\theta} - \tilde{L}_h)^{-1} \tilde{L}_h^{1/2}\|_{L(L^2(\mathcal{S}))} \lesssim h^{\beta-\delta-1}. \quad (71)$$

Similarly, using $T_h = L_h^{-1} \Lambda_h$ and the boundedness of Λ_h , we obtain

$$\begin{aligned} R^{1-\beta/2} \|\tilde{L}_h^{3/2} (Re^{i\theta} - L_h)^{-1} T_h\|_{L(L^2(\mathcal{S}))} &= R^{1-\beta/2} \|L_h^{1/2} (Re^{i\theta} - L_h)^{-1} \Lambda_h\|_{L(L^2(\mathcal{S}))} \\ &\lesssim R^{1-\beta/2} \sup_{\lambda \in \sigma(L_h)} \frac{\lambda^{1/2}}{|Re^{i\theta} - \lambda|} \leq R^{1-\beta/2} \frac{(Ch^{-2})^{1/2}}{h^{-2} |(C+1)e^{i\theta} - C|} \lesssim h^{\beta-1}. \end{aligned}$$

Therefore, by (70), (71), and the preceding estimate,

$$R^{1-\beta} \|\tilde{L}_h^{\delta/2} \mathcal{I}_2\|_{L(L^2(\mathcal{S}))} \lesssim h^2 h^{\beta-\delta-1} h^{\beta-1} = h^{2\beta-\delta}.$$

Since the bound is uniform in θ , integration over $[-\pi, \pi]$ gives

$$R^{1-\beta} \int_{-\pi}^{\pi} \|\tilde{L}_h^{\delta/2} \mathcal{I}_2\|_{L(L^2(\mathcal{S}))} d\theta \lesssim h^{2\beta-\delta}. \quad (72)$$

Finally, we consider the small circular arc. Since r is fixed independently of h and lies strictly below the spectra of both \tilde{L}_h and L_h , the resolvents $(re^{i\theta} - \tilde{L}_h)^{-1}$ and $(re^{i\theta} - L_h)^{-1}$

are uniformly bounded in $L(V_h)$ for $\theta \in [-\pi, \pi]$. Therefore, arguing exactly as for \mathcal{I}_2 , but now with r fixed instead of $R \approx h^{-2}$, we obtain

$$r^{1-\beta} \int_{-\pi}^{\pi} \|\tilde{L}_h^{\delta/2} \mathcal{I}_3\|_{L(L^2(\mathcal{S}))} d\theta \lesssim h^2. \quad (73)$$

Indeed, in this case all resolvent factors remain uniformly bounded, and the only h -dependence comes from the factor h^2 arising from (65).

Substituting (69), (72), and (73) into (62), we conclude that

$$\|E_3\|_{\delta} \lesssim h^{\min\{2\beta-\delta, 2\}} \left(\log \frac{1}{h}\right)^{[2\beta-\delta=2]} \|f\|. \quad (74)$$

The estimate for E_2 is obtained by the same contour argument, now replacing the pair (\tilde{L}_h, L_h) by (\hat{L}_h, \tilde{L}_h) . Since both operators are realized in the exact L^2 inner product, no projection mismatch occurs, and the role of (65) is played by Lemma 4.1. Thus

$$\|E_2\|_{\delta} \lesssim h^{\min\{2\beta-\delta, 2\}} \left(\log \frac{1}{h}\right)^{[2\beta-\delta=2]} \|f\|. \quad (75)$$

Combining (57), (75), and (74) in (56), we obtain

$$\|u_{\beta} - \bar{u}_{\beta, h}\|_{\delta} \lesssim h^{\min\{2\beta-\delta, 2\}} \left(\log \frac{1}{h}\right)^{[2\beta-\delta=2, \delta>0]} \|f\|.$$

Finally, in the case $\delta = 0$ and $2\beta = 2$, one has $\beta = 1$. Then the logarithmic factor disappears, because both perturbation terms are of order h^2 by Lemma 4.1. This proves the theorem. \square

Proof of Theorem 4.4 from the main text. Following the notation of the proof of Theorem 4.3, it is enough to estimate the analogue of E_3 . Let $g = L^{\sigma/2} f \in L^2(\mathcal{S})$. Then $f = L^{-\sigma/2} g$, $\|g\| = \|f\|_{\sigma}$, and therefore

$$E_3^{(\sigma)} := \left\| (\tilde{L}_h^{-\beta} \Pi_h - L_h^{-\beta} \Lambda_h) L^{-\sigma/2} g \right\|_{\delta}.$$

We add and subtract $(\tilde{L}_h^{-\beta} \Pi_h - L_h^{-\beta} \Lambda_h) \tilde{L}_h^{-\sigma/2} \Pi_h g$ and use the triangle inequality:

$$\begin{aligned} E_3^{(\sigma)} &\leq \left\| (\tilde{L}_h^{-\beta} \Pi_h - L_h^{-\beta} \Lambda_h) (L^{-\sigma/2} - \tilde{L}_h^{-\sigma/2} \Pi_h) g \right\|_{\delta} \\ &\quad + \left\| (\tilde{L}_h^{-\beta} \Pi_h - L_h^{-\beta} \Lambda_h) \tilde{L}_h^{-\sigma/2} \Pi_h g \right\|_{\delta}. \end{aligned} \quad (76)$$

We begin with the first term. By Theorem 4.3, applied with right-hand side

$$(L^{-\sigma/2} - \tilde{L}_h^{-\sigma/2} \Pi_h) g,$$

we obtain

$$\begin{aligned} &\left\| (\tilde{L}_h^{-\beta} \Pi_h - L_h^{-\beta} \Lambda_h) (L^{-\sigma/2} - \tilde{L}_h^{-\sigma/2} \Pi_h) g \right\|_{\delta} \\ &\lesssim h^{\min\{2\beta-\delta, 2\}} \left(\log \frac{1}{h}\right)^{[2\beta-\delta=2]} \left\| (L^{-\sigma/2} - \tilde{L}_h^{-\sigma/2} \Pi_h) g \right\|. \end{aligned} \quad (77)$$

Now, the classical finite element estimate for fractional powers gives

$$\left\| (L^{-\sigma/2} - \tilde{L}_h^{-\sigma/2} \Pi_h) g \right\| \lesssim h^{\sigma} \|g\|.$$

Substituting this into (77), we find

$$\begin{aligned} & \left\| (\tilde{L}_h^{-\beta} \Pi_h - L_h^{-\beta} \Lambda_h) (L^{-\sigma/2} - \tilde{L}_h^{-\sigma/2} \Pi_h) g \right\|_{\delta} \\ & \lesssim h^{\min\{2\beta-\delta, 2\}+\sigma} \left(\log \frac{1}{h} \right)^{[2\beta-\delta=2]} \|g\|. \end{aligned} \quad (78)$$

We now turn to the second term in (76). As in the proof of Theorem 4.3, we use the contour representation of the fractional power. Thus it suffices to estimate

$$\left\| L_h^{\delta/2} (\tilde{L}_h^{-\beta} \Pi_h - L_h^{-\beta} \Lambda_h) \tilde{L}_h^{-\sigma/2} \Pi_h \right\|_{L(L^2(\mathcal{S}))}.$$

Proceeding exactly as before, the analogue of (63) now gives

$$\begin{aligned} \mathcal{I}_1 &= t(t + \tilde{L}_h)^{-1} \tilde{L}_h (\tilde{L}_h^{-1} - L_h^{-1}) L_h (t + L_h)^{-1} T_h \tilde{L}_h^{-\sigma/2} \\ &= t(t + \tilde{L}_h)^{-1} \tilde{L}_h^{1/2} \tilde{L}_h^{1/2} (\tilde{L}_h^{-1} - L_h^{-1}) L_h (t + L_h)^{-1} T_h \tilde{L}_h^{-\sigma/2}. \end{aligned}$$

Using (65), we obtain

$$\begin{aligned} \left\| L_h^{\delta/2} \mathcal{I}_1 \right\|_{L(L^2(\mathcal{S}))} &\lesssim h^2 t \left\| L_h^{\delta/2} (t + L_h)^{-1} L_h^{1/2} \right\|_{L(L^2(\mathcal{S}))} \\ &\quad \times \left\| \tilde{L}_h^{3/2} (t + \tilde{L}_h)^{-1} T_h \tilde{L}_h^{-\sigma/2} \right\|_{L(L^2(\mathcal{S}))}. \end{aligned} \quad (79)$$

By the spectral theorem,

$$\left\| L_h^{\delta/2} (t + L_h)^{-1} L_h^{1/2} \right\|_{L(L^2(\mathcal{S}))} = \sup_{\lambda \in \sigma(L_h)} \frac{\lambda^{\frac{1}{2} + \frac{\delta}{2}}}{t + \lambda} \lesssim t^{\frac{\delta}{2} - \frac{1}{2}}, \quad (80)$$

and similarly

$$\begin{aligned} \left\| \tilde{L}_h^{3/2} (t + \tilde{L}_h)^{-1} T_h \tilde{L}_h^{-\sigma/2} \right\|_{L(L^2(\mathcal{S}))} &= \left\| \tilde{L}_h^{1/2} (t + \tilde{L}_h)^{-1} \Pi_h \tilde{L}_h^{-\sigma/2} \right\|_{L(L^2(\mathcal{S}))} \\ &\lesssim \sup_{\lambda \in \sigma(\tilde{L}_h)} \frac{\lambda^{\frac{1}{2} - \frac{\sigma}{2}}}{t + \lambda} \lesssim t^{-\frac{1}{2} - \frac{\sigma}{2}}. \end{aligned} \quad (81)$$

Substituting (80) and (81) into (79), we get

$$\left\| L_h^{\delta/2} \mathcal{I}_1 \right\|_{L(L^2(\mathcal{S}))} \lesssim h^2 t^{\frac{\delta-\sigma}{2}}.$$

Therefore

$$\begin{aligned} \int_r^R t^{-\beta} \left\| L_h^{\delta/2} \mathcal{I}_1 \right\|_{L(L^2(\mathcal{S}))} dt &\lesssim h^2 \int_r^R t^{-\beta + \frac{\delta-\sigma}{2}} dt \\ &\lesssim h^{\min\{2\beta+\sigma-\delta, 2\}} \left(\log \frac{1}{h} \right)^{[2\beta+\sigma-\delta=2]}. \end{aligned} \quad (82)$$

We next estimate the contribution on the large circular arc. As in the proof of Theorem 4.3, the corresponding resolvent term satisfies

$$\begin{aligned} \left\| L_h^{\delta/2} \mathcal{I}_2 \right\|_{L(L^2(\mathcal{S}))} &\lesssim h^2 R \left\| L_h^{\delta/2} (Re^{i\theta} - L_h)^{-1} L_h^{1/2} \right\|_{L(L^2(\mathcal{S}))} \\ &\quad \times \left\| \tilde{L}_h^{3/2} (Re^{i\theta} - \tilde{L}_h)^{-1} T_h \tilde{L}_h^{-\sigma/2} \right\|_{L(L^2(\mathcal{S}))}. \end{aligned} \quad (83)$$

Using again the spectral theorem and the fact that $R = (C+1)h^{-2}$ lies a fixed relative distance away from the spectra, we obtain

$$R^{1-\beta/2} \left\| L_h^{\delta/2} (Re^{i\theta} - L_h)^{-1} L_h^{1/2} \right\|_{L(L^2(\mathcal{S}))} \lesssim h^{\beta-\delta-1},$$

and

$$R^{1-\beta/2} \|\tilde{L}_h^{3/2} (Re^{i\theta} - \tilde{L}_h)^{-1} T_h \tilde{L}_h^{-\sigma/2}\|_{L(L^2(\mathcal{S}))} \lesssim h^{\beta+\sigma-1}.$$

Therefore

$$R^{1-\beta} \int_{-\pi}^{\pi} \|L_h^{\delta/2} \mathcal{I}_2\|_{L(L^2(\mathcal{S}))} d\theta \lesssim h^{2\beta+\sigma-\delta}. \quad (84)$$

Finally, on the small circular arc, the argument is simpler because r is fixed independently of h . As before, all resolvent factors remain uniformly bounded, and the only h -dependence comes from the factor h^2 in (65). Thus

$$r^{1-\beta} \int_{-\pi}^{\pi} \|L_h^{\delta/2} \mathcal{I}_3\|_{L(L^2(\mathcal{S}))} d\theta \lesssim h^2. \quad (85)$$

Combining (82), (84), and (85), we conclude that

$$E_3^{(\sigma)} \lesssim h^{\min\{2\beta+\sigma-\delta, 2\}} \left(\log \frac{1}{h}\right)^{[2\beta+\sigma-\delta=2]} \|g\|. \quad (86)$$

Together with (78), this yields

$$E_3^{(\sigma)} \lesssim h^{\min\{2\beta+\sigma-\delta, 2\}} \left(\log \frac{1}{h}\right)^{[2\beta+\sigma-\delta=2]} \|g\|.$$

Indeed, the bound in (78) is already of the required order. If $2\beta - \delta \neq 2$, then this follows immediately by comparing the powers of h . If $2\beta - \delta = 2$, one has

$$h^{2+\sigma} \log \frac{1}{h} \lesssim h^2,$$

since $h^\sigma \log(1/h)$ remains bounded as $h \rightarrow 0$. Therefore,

$$h^{\min\{2\beta-\delta, 2\}+\sigma} \left(\log \frac{1}{h}\right)^{[2\beta-\delta=2]} \lesssim h^{\min\{2\beta+\sigma-\delta, 2\}},$$

and hence the first term in (76) is controlled by the same rate as in (86).

Since $\|g\| = \|f\|_\sigma$, the same bound holds with $\|f\|_\sigma$ on the right-hand side. The term analogous to E_2 is treated exactly as in the proof of Theorem 4.3, replacing the pair (\tilde{L}_h, L_h) by $(\tilde{L}_h, \tilde{L}_h)$. Since both operators are realized in the exact L^2 inner product, no projection mismatch occurs, and the resulting estimate is no worse than the one above. The classical FEM estimate for smoother data gives the result to the term analogous to E_1 . The proof is concluded by combining the three estimates. \square

Proof of Theorem 4.6 from the main text. By Theorem 4.4, it is enough to estimate

$$\|u_{\beta,h} - \bar{u}_{\beta,h}\|_\delta.$$

Set

$$d_h := L_h^{-\beta+\delta/2} (P_h - \Lambda_h) f.$$

Since, on V_h , the norm $\|\cdot\|_\delta$ is equivalent to the graph norm induced by $L_h^{\delta/2}$, with constants independent of h , it is enough to estimate $\|d_h\|$.

We first consider the case $\sigma = 0$. Let $g \in L^2(\mathcal{S})$ be arbitrary. Since $\Lambda_h g \in V_h$ and

$$\langle \Lambda_h g, \chi \rangle_h = (g, \chi), \quad \chi \in V_h,$$

we have

$$(d_h, g) = \langle d_h, \Lambda_h g \rangle_h.$$

Using the selfadjointness of L_h with respect to $\langle \cdot, \cdot \rangle_h$, we obtain

$$(d_h, g) = \langle (P_h - \Lambda_h)f, L_h^{-\beta+\delta/2} \Lambda_h g \rangle_h.$$

By the definitions of P_h and Λ_h ,

$$\langle P_h f, \chi \rangle_h = (f, Q\chi), \quad \langle \Lambda_h f, \chi \rangle_h = (f, \chi), \quad \chi \in V_h.$$

Therefore

$$(d_h, g) = (f, QL_h^{-\beta+\delta/2} \Lambda_h g) - (f, L_h^{-\beta+\delta/2} \Lambda_h g) = (f, (Q - I)L_h^{-\beta+\delta/2} \Lambda_h g).$$

Hence

$$|(d_h, g)| \leq \|f\| \|(Q - I)L_h^{-\beta+\delta/2} \Lambda_h g\|.$$

Taking the supremum over all $g \in L^2(\mathcal{S})$ with $\|g\| = 1$, we conclude that

$$\|d_h\| \lesssim \|(Q - I)L_h^{-\beta+\delta/2} \Lambda_h\|_{L(L^2(\mathcal{S}))} \|f\|. \quad (87)$$

Since Q is the nodal interpolation onto dual-cell constants, we have

$$\|(I - Q)\chi\| \lesssim h\|\chi\|_{H^1(\mathcal{S})}, \quad \chi \in V_h.$$

Therefore,

$$\|d_h\| \lesssim h \|L_h^{-\beta+\delta/2} \Lambda_h\|_{L(L^2(\mathcal{S}); H^1(\mathcal{S}))} \|f\|. \quad (88)$$

Observe that since

$$\|L_h^{-\beta+\delta/2} \Lambda_h g\|_{H^1(\mathcal{S})} \lesssim \|L_h^{-\beta+\delta/2} \Lambda_h g\|_{1,h},$$

it is enough to estimate the discrete norm on the right. Applying Proposition 4.2 from the main text with

$$r = -2\beta + \delta + 1, \quad s = 0,$$

to $\chi = \Lambda_h g$, we obtain

$$\begin{aligned} \|L_h^{-\beta+\delta/2} \Lambda_h g\|_{1,h} &= \|\Lambda_h g\|_{-2\beta+\delta+1,h} \lesssim h^{-(2\beta+\delta+1)^+} \|\Lambda_h g\| \\ &\lesssim h^{\min\{2\beta-\delta, 1\}-1} \|\Lambda_h g\|. \end{aligned}$$

where we used in the last inequality that for every $a, b \in \mathbb{R}$ we have that $(a+b)^+ = b - \min\{-a, b\}$. Plugging the last inequality into (88), we obtain

$$\|d_h\| \lesssim h^{\min\{2\beta-\delta, 1\}} \|f\|.$$

We now consider the case $0 < \sigma \leq 1$. Let $g \in L^2(\mathcal{S})$ and let $w \in \mathcal{V}$ solve the adjoint problem

$$Lw = g.$$

By convexity of \mathcal{S} and elliptic regularity, we have $w \in H^2(\mathcal{S})$ and

$$\|w\|_{H^2(\mathcal{S})} \lesssim \|g\|.$$

Let $w_h = R_h w \in V_h$ be the Ritz projection of w , that is,

$$a_h(w_h, \chi) = a(w, \chi), \quad \chi \in V_h.$$

We first record the estimate

$$\|w_h\|_{2,h} \lesssim \|w\|_{H^2(\mathcal{S})} + h\|w_h\|_{H^1(\mathcal{S})} \lesssim \|g\|, \quad (89)$$

for $h \leq 1$. Indeed, for every $\chi \in V_h$,

$$\langle L_h w_h, \chi \rangle_h = a_h(w_h, \chi) = a(w, \chi) - (a - a_h)(w_h, \chi).$$

Hence

$$|\langle L_h w_h, \chi \rangle_h| \lesssim \|Lw\| \|\chi\| + h^2 \|w_h\|_{H^1(\mathcal{S})} \|\chi\|_{H^1(\mathcal{S})}.$$

Taking the supremum over $\chi \in V_h$, and using the inverse inequality together with the H^1 -stability of the Ritz projection, gives the first bound in (89). The second follows from elliptic regularity and H^1 -stability of the Ritz projection, by the estimate

$$\|w_h\|_{H^1(\mathcal{S})} \lesssim \|w\|_{H^1(\mathcal{S})} \lesssim \|w\|_{H^2(\mathcal{S})} \lesssim \|g\|.$$

We now estimate d_h by duality. Using the definition of d_h and the fact that $Lw = g$, we compute

$$\begin{aligned} (g, d_h) &= a(d_h, w) \\ &= a(d_h, w_h) - a_h(d_h, w_h) + a_h(d_h, w_h) \\ &= a(d_h, w_h) - a_h(d_h, w_h) + \left(f, (I - Q)L_h^{-\beta+\delta/2+1} w_h \right). \end{aligned} \tag{90}$$

We estimate the two terms separately. For the first one, Definition 2.5 from the main text gives

$$|a(d_h, w_h) - a_h(d_h, w_h)| \lesssim h^2 |d_h|_1 |w_h|_1.$$

Now, use the estimate for $\sigma = 0$ that we proved in the first part, but now applied to

$$L_h^{1/2} d_h = L_h^{-\beta+\delta/2+1/2} (P_h - \Lambda_h) f,$$

to obtain

$$|d_h|_1 \lesssim h^{\min\{2\beta-\delta-1, 1\}} \|f\|.$$

Therefore

$$\begin{aligned} |a(d_h, w_h) - a_h(d_h, w_h)| &\lesssim h^2 h^{\min\{2\beta-\delta-1, 1\}} \|f\| \|w_h\|_{H^1(\mathcal{S})} \\ &\lesssim h^{\min\{2\beta-\delta+1, 3\}} \|f\|_\sigma \|g\|. \end{aligned} \tag{91}$$

For the second term in (90), Lemma 4.5 from the main text gives

$$\left| \left(f, (I - Q)L_h^{-\beta+\delta/2+1} w_h \right) \right| \lesssim h^{1+\sigma} \|f\|_\sigma \|L_h^{-\beta+\delta/2+1} w_h\|_{H^1(\mathcal{S})}. \tag{92}$$

We again use Proposition 4.2 from the main text. Since

$$\|L_h^{-\beta+\delta/2+1} w_h\|_{H^1(\mathcal{S})} \lesssim \|L_h^{-\beta+\delta/2+1} w_h\|_{1,h},$$

applying Proposition 4.2 from the main text with

$$r = 1, \quad s = 2,$$

to $\chi = L_h^{-\beta+\delta/2+1} w_h$ yields

$$\|L_h^{-\beta+\delta/2+1} w_h\|_{1,h} \lesssim h^{-(1-2)^+} \|L_h^{-\beta+\delta/2+1} w_h\|_{2,h}.$$

Equivalently, after shifting the indices by $-\beta + \delta/2 + 1$, we obtain

$$\|L_h^{-\beta+\delta/2+1} w_h\|_{H^1(\mathcal{S})} \lesssim h^{\min\{2\beta-\delta, 1\}-1} \|w_h\|_{2,h}.$$

Substituting this into (92) and then using (89), we find

$$\begin{aligned} \left| \left(f, (I - Q)L_h^{-\beta+\delta/2+1}w_h \right) \right| &\lesssim h^{1+\sigma} h^{\min\{2\beta-\delta,1\}-1} \|w_h\|_{2,h} \|f\|_\sigma \\ &\lesssim h^{\min\{2\beta+\sigma-\delta,1+\sigma\}} \|f\|_\sigma \|g\|. \end{aligned} \quad (93)$$

Substituting (91) and (93) into (90), we obtain

$$|(g, d_h)| \lesssim h^{\min\{2\beta+\sigma-\delta,1+\sigma\}} \|f\|_\sigma \|g\|.$$

Since this holds for every $g \in L^2(\mathcal{S})$, duality gives

$$\|d_h\| \lesssim h^{\min\{2\beta+\sigma-\delta,1+\sigma\}} \|f\|_\sigma.$$

Recalling that $\|u_{\beta,h} - \bar{u}_{\beta,h}\|_\delta \lesssim \|d_h\|$, the result follows. \square

References

- [1] K. J. R. ALMEIDA-SOUSA, D. BOLIN, AND A. B. SIMAS, *fractional_box_experiments*. https://github.com/KJhonson/fractional_box_experiments, 2026. Accessed: 2026-05-10.
- [2] R. E. BANK AND D. J. ROSE, *Some error estimates for the box method*, SIAM Journal on Numerical Analysis, 24 (1987), pp. 777–787, <https://doi.org/10.1137/0724050>.
- [3] D. BOLIN AND K. KIRCHNER, *The rational spde approach for gaussian random fields with general smoothness*, Journal of Computational and Graphical Statistics, 29 (2020), pp. 274–285.
- [4] D. BOLIN, A. B. SIMAS, AND Z. XIONG, *Covariance-based rational approximations of fractional spdes for computationally efficient bayesian inference*, Journal of Computational and Graphical Statistics, 33 (2024), pp. 64–74, <https://doi.org/10.1080/10618600.2023.2231051>.
- [5] A. BONITO AND J. PASCIAK, *Numerical approximation of fractional powers of elliptic operators*, Mathematics of Computation, 84 (2015), pp. 2083–2110, <https://doi.org/10.1090/S0025-5718-2015-02937-8>.
- [6] S. C. BRENNER AND L. R. SCOTT, *The Mathematical Theory of Finite Element Methods*, Springer New York, New York, NY, 2008, <https://doi.org/10.1007/978-0-387-75934-0>.
- [7] L. CAFFARELLI AND L. SILVESTRE, *An extension problem related to the fractional laplacian*, Communications in partial differential equations, 32 (2007), pp. 1245–1260.
- [8] P. CHATZIPANTELIDIS, *Finite volume methods for elliptic pde’s: a new approach*, ESAIM: Mathematical Modelling and Numerical Analysis, 36 (2002), pp. 307–324, <https://doi.org/10.1051/m2an:2002014>.
- [9] S.-H. CHOU AND Q. LI, *Error estimates in L^2, H^1 and L^∞ in covolume methods for elliptic and parabolic problems: a unified approach*, Mathematics of Computation, 69 (2000), pp. 103–120, <https://doi.org/10.1090/S0025-5718-99-01192-8>.
- [10] P. G. CIARLET, *The finite element method for elliptic problems*, SIAM, 2002.

- [11] S. G. COX AND K. KIRCHNER, *Regularity and convergence analysis in sobolev and hölder spaces for generalized whittle–matérn fields*, *Numerische Mathematik*, 146 (2020), pp. 819–873, <https://doi.org/10.1007/s00211-020-01151-x>.
- [12] Q. DU, M. GUNZBURGER, R. B. LEHOUCQ, AND K. ZHOU, *Numerical methods for non-local and fractional models*, *Acta Numerica*, 29 (2020), pp. 1–124.
- [13] R. E. EWING, T. LIN, AND Y. LIN, *On the accuracy of the finite volume element method based on piecewise linear polynomials*, *SIAM Journal on Numerical Analysis*, 39 (2002), pp. 1865–1888, <https://doi.org/10.1137/s0036142900368873>, <http://dx.doi.org/10.1137/s0036142900368873>.
- [14] G. J. FIX, *Effects of quadrature errors in finite element approximation of steady state, eigenvalue and parabolic problems*, in *The Mathematical Foundations of the Finite Element Method with Applications to Partial Differential Equations*, A. Aziz, ed., Academic Press, 1972, pp. 525–556, <https://doi.org/https://doi.org/10.1016/B978-0-12-068650-6.50024-1>, <https://www.sciencedirect.com/science/article/pii/B9780120686506500241>.
- [15] H. FUJITA AND T. SUZUKI, *Evolution problems*, Elsevier, 1991, pp. 789–928, [https://doi.org/10.1016/s1570-8659\(05\)80043-2](https://doi.org/10.1016/s1570-8659(05)80043-2), [http://dx.doi.org/10.1016/s1570-8659\(05\)80043-2](http://dx.doi.org/10.1016/s1570-8659(05)80043-2).
- [16] C. GLUSA AND E. OTÁROLA, *Error estimates for the optimal control of a parabolic fractional pde*, *SIAM Journal on Numerical Analysis*, 59 (2021), pp. 1140–1165.
- [17] M. HAASE, *The Functional Calculus for Sectorial Operators*, Birkhäuser Basel, Basel, 2006, <https://doi.org/10.1007/3-7643-7698-8>.
- [18] W. HACKBUSCH, *On first and second order box schemes*, *Computing*, 41 (1989), pp. 277–296.
- [19] S. HARIZANOV, R. LAZAROV, P. MARINOV, J. PASCIAK, AND P. VASSILEVSKI, *Numerical approximation of fractional powers of elliptic operators*, *IMA Journal of Numerical Analysis*, 40 (2020), pp. 1746–1792.
- [20] S. HÖLLBACHER AND G. WITTUM, *A sharp interface method using enriched finite elements for elliptic interface problems*, *Numerische Mathematik*, 147 (2021), pp. 759–781.
- [21] H. JIANGUO AND X. SHITONG, *On the finite volume element method for general self-adjoint elliptic problems*, *SIAM journal on numerical analysis*, 35 (1998), pp. 1762–1774, <https://doi.org/10.1137/S0036142994264699>.
- [22] B. JIN AND Z. ZHOU, *Numerical Treatment and Analysis of Time-Fractional Evolution Equations*, Springer International Publishing, 2023, <https://doi.org/10.1007/978-3-031-21050-1>, <http://dx.doi.org/10.1007/978-3-031-21050-1>.
- [23] S. LIANG, X. MA, AND A. ZHOU, *Finite volume methods for eigenvalue problems*, *BIT Numerical Mathematics*, 41 (2001), pp. 345–363, <https://doi.org/10.1023/A:1021946607960>, <https://doi.org/10.1023/A:1021946607960>.
- [24] F. LINDGREN, H. RUE, AND J. LINDSTRÖM, *An explicit link between gaussian fields and gaussian markov random fields: the stochastic partial differential equation approach*, *Journal of the Royal Statistical Society Series B: Statistical Methodology*, 73 (2011), pp. 423–498, <https://doi.org/10.1111/j.1467-9868.2011.00777.x>.

- [25] P. R. STINGA AND J. L. TORREA, *Regularity theory and extension problem for fractional nonlocal parabolic equations and the master equation*, SIAM Journal on Mathematical Analysis, 49 (2017), pp. 3893–3924.
- [26] G. STRANG AND G. FIX, *An Analysis of the Finite Element Methods, New Edition*, Wellesley-Cambridge Press, Philadelphia, PA, 2008, <https://doi.org/10.1137/1.9780980232707>, <https://epubs.siam.org/doi/abs/10.1137/1.9780980232707>, <https://arxiv.org/abs/https://epubs.siam.org/doi/pdf/10.1137/1.9780980232707>.
- [27] V. THOMÉE, *Galerkin Finite Element Methods for Parabolic Problems*, Springer Berlin Heidelberg, Berlin, Heidelberg, 2006, https://doi.org/10.1007/3-540-33122-0_15.
- [28] Y. VOET, E. SANDE, AND A. BUFFA, *A mathematical theory for mass lumping and its generalization with applications to isogeometric analysis*, Computer Methods in Applied Mechanics and Engineering, 410 (2023), p. 116033, <https://doi.org/10.1016/j.cma.2023.116033>.